OsloMet – Oslo Metropolitan Univesity

Department of Civil Engineering and Energy Technolgly
Mailing address: PB 4 St. Olavs plass, N-0130 Oslo, Norway
Street addresse: Pilestredet 35, Oslo

Phone: 67 23 50 00
www.hioa.no

BACHELORS THESIS

TITLE CFD analysis of displacement ventilation	DATE 23.05.1018
	NUMBER OF PAGES/ATTACHEMENTS 53
AUTHORS Faical Lambarki Jan Andreas Cacal Taftø Mahamud Hussein Dahir	SUPERVISOR Arnab Chaudhuri

DONE IN COLLABORATION WITH	CONTACT

ABSTRACT
Displacement ventilation is an air supply method that uses supplied air near the floor at low velocity and fewer degrees below the air in the room. Well-designed displacement ventilation gives sufficient air quality, thermal comfort in the occupied zone as well as energy saving since free cooling can be used.

The problem that was introduced to us was that laboratory measurements and CFD simulations have had inconclusive results in regards to the correctness of the Archimedes number proposed in the Nordtest method NT VVS 083. STAR-CCM+ has been used in this study to conduct simulations concerning this problem. With varying diffuser heights, inlet flow rates and heat loads, there were no significant changes in the Archimedes number. However, this was done with 20% increment of diffuser height. Further research is required to determine if the Archimedes number should include a length scale for diffuser height.

3 KEYWORDS
Displacement ventilation
Gravity current
CFD

Project Description

Displacement ventilation is a potentially excellent means of air distribution in building ventilation, especially in rooms with relatively high occupancy density. However, compared to the conventional mixing ventilation, displacement ventilation systems is more difficult to design/dimension. This is partly because equations describing jet theory in dimensioning supply air terminals with high jet momentum are well established, whilst there have been no equivalent reliable equations explaining the air speed in displacement ventilation. The risk of cold draught near the floor has been one of the main reasons why the interest in displacement ventilation in Scandinavia has dwindled in recent years. However, it is slowly becoming more popular internationally and even more so in Norway with the emergence of ZEB (Zero Emission Buildings) with extreme energy-efficiency (e.g. Powerhouse Kjørbo located in Sandvika, just outside of Oslo).

Based on the theory by Prof.em. Eimund Skåret, semi-emperical equations for designing displacement ventilation were proposed. However, laboratory measurements carried out to validate the equations did not give definitive confirmation of the correctness of the form of the Archimedes number. Should the Archimedes number include a length scale for diffuser height?

The following tasks are to be considered:

A) Validate CFD models for ventilations systems with laboratory measurements.

B) Conduct literature review on CFD modeling and computing near-zone velocity of DV with boundary conditions, turbulence models and grid refinement.

C) Build Three-Dimensional CFD models for DV following the guidelines and dimensions of Nordtest NT VVS 083:A with heat source.

Acknowledgement

We would like to thank our supervisor Arnab Chaudhuri for the excellent guidance and encouragement throughout this thesis. He has been of tremendous assistance and contribution with the knowledge in this field. We would also like to recognize and appreciate the help given by Ole Melhus for his guidance on the use of STAR CCM + and understanding of CFD modelling in general. We would also like to thank Peter Schild for proposing this bachelors thesis to us, and his guidance with relevant literature on studies done earlier.

Faical Lambarki   Jan Andreas Cacal Taftø   Mahamud Hussein Dahir

Date: 23 MAY 2018

Place: OSLO

Abstract

Displacement ventilation is an air supply method that uses supplied air near the floor at low velocity and fewer degrees below the air in the room. Well-designed displacement ventilation gives sufficient air quality, thermal comfort in the occupied zone as well as energy saving since free cooling can be used.

Several simulations were carried out using numerical techniques in STAR CCM+. A benchmark case study using a 2D simulation of a mixed ventilation system was carried out to investigate and compare the flow patterns with existing experimental data. A grid-independence test was performed by generating different computational grids. Results showed that the finer mesh gave better and more stable results than coarse mesh. Different turbulence models were also tested to predict the velocity distribution in the room. The results found in this section correspond very well with benchmark tests done.

A three-dimensional case study of displacement ventilation was also carried out to investigate the flow of the flow in a room with a heat source. A water-box model with water as the working fluid was used in this simulation. Both steady and unsteady state simulation with different heat load were run and results obtained were compared to measurement and numerical results in existing literature. The general characteristic of a 3D displacement ventilation was presented in these simulation. Results found were also found to be in good agreement with those in the literature.

The last section presents the main objective of this bachelors thesis. The problem that was introduced to us was that laboratory measurements and CFD simulations have had inconclusive results in regards to the correctness of the Archimedes number proposed in the Nordtest method NT VVS 083. STAR-CCM+ has been used in this study to conduct simulations concerning this problem. With varying diffuser heights, inlet flow rates and heat loads, there were no significant changes in the Archimedes number. However, this was done with 20% increment of diffuser height. Further research is required to determine if the Archimedes number should include a length scale for diffuser height.

Contents

1 Introduction

1.1 Background

Displacement ventilation is a potentially excellent means of air distribution in building ventilation, especially in rooms with relatively high occupancy density. However, compared to the conventional mixing ventilation, displacement ventilation systems is more difficult to design/dimension. This is partly because of well established equations describing jet theory in dimensioning supply air terminals with high jet momentum, whilst there have been no equivalent reliable equations explaining the air speed in displacement ventilation. With the risk of cold draught near the floor, very careful design is needed for successful results, and this has been one of the main reasons why the interest in displacement ventilation in Scandinavia has dwindled in recent years. However, it is slowly becoming more popular internationally and even more so in Norway with the emergence of ZEB (Zero Emission Buildings) with extreme energy-efficiency (e.g. Powerhouse Kjørbo).

Fresh air is distributed at low velocity at lower heights and at a temperature lower in relation to the room. This supply is usually at floor level, directly in the occupied zone and is drawn to heat loads by vertically created convectional currents. The system also operates at very low pressure thus reducing the noise in the occupied area. Temperature stratification zones are created in spaces in the room. This way, contaminant air is carried out from the occupied zones towards the high point of the room.

In 2003 an international standard called Nordtest NT VVS 083 was presented. Based on the theory of Prof.em. Eimund Skåret this standard proposed suitable semi-empirical equations for designing displacement ventilation. The equations enable the HVAC engineer to calculate the air speed at any position on the floor, for any given supply flow rate, any supply temperature, and any size of diffuser (for a series of geometrically similar by different-sized diffusers). Each series of geometrically similar displacement ventilation diffusers has its own set of empirical coefficients. The empirical coefficients are found by correlation with laboratory measurements, and can be given in the manufacturer's product brochure, or the manufacturer can generate tables or charts based on the theory. The equations are rather simple in form, and contain only two variable parameters, namely Buoyancy flux, B, and Archimedes number, Ar, (analogous to Richardson number in this case). Separate sets of equations apply to radial and linear diffusers. Laboratory studies carried out to validate these equations did not give definitive confirmation of the correctness of the form of the Archimedes number. Should the Archimedes number include a length scale for diffuser height?

1.2 Objective

The focus of this study is to determine the effects the height of diffuser and volumetric flow rate on a DV system. Numerical simulations will be performed using a commercial CFD tool. The advantages of using CFD over experiments are lower cost and less resources. The project has been brought forward by the need to conduct further research in order to validate the proposed equations for the simplified Archimedes number by Professor Eimund Skåret.

The objectives of the present study are:

1. Conduct literature review on recommendations about CFD modeling and computing near-zone velocity of DV with boundary conditions, turbulence models and grid refinement.

2. Validate CFD models for ventilations systems with laboratory measurements.

3. Build Three-Dimensional CFD models for DV following the guidelines and dimensions of Nordtest NT VVS 083:A with heat source. This includes conducting simulations to evaluate maximum velocity at different positions from the diffuser.

2 Theory and Literature review

2.1 Ventilation in buildings

Ventilation helps in controlling the indoor climate thus better health and comfort. A good ventilation system is one that enhances a good working environment and increase in productivity. The principle of a good ventilation system can also be used in homes since on average we spend 90 percent of the time indoors. [1]

Ventilation systems have among others the following importance;

- Reduces condensation that can be a decaying factor to the building structure.

- Reduces risks of allergies by trapping and filtering allergens such as pollen and dust.

- Lowers concentrations of dangerous gases which has been linked to lung cancer or other physical ailments.

- Reduces volatile organic compounds emitted from household chemicals and furnishings.

- Reduce back-drafting risks.

- Removes and replaces excessive heat with fresh air in order to obtain a higher air quality.

- Reduces the buildings energy consumption.

2.2 Air distribution systems and design method

Ventilation systems are characterized according to the method of supply, the forces which drive it and the flow type of the supply air. There are two main design systems of air distribution namely;

- Mixing ventilation

- Displacement ventilation (DV)

Mixing ventilation is a system whereby the air is supplied through a small opening near (or in) the ceiling at relatively high velocity where a uniformed environment in regards of air concentration and thermal comfort is achieved. The above system uses momentum forces to push and mix the supply air with the contaminated air as the outdoor air is supplied far from the occupant zone. The high air velocity is necessary to mix with a large amount of the air in the room. During the first air flow cycle the air velocity will be high, but as the

quantity of room air that becomes mixed increases, the air velocity can be decreased. The supply fluid then reaches the occupied zone depending on the velocity at the supply. The occupied zone is estimated to be 1.80 cm above the floor and is an essential element to consider when designing a mixing ventilation system in order to avoid draught which can be caused by the jet flow from the diffuser at the ceiling. Figure 1 shows a schematic of such a system using a ceiling based diffuser.[2]
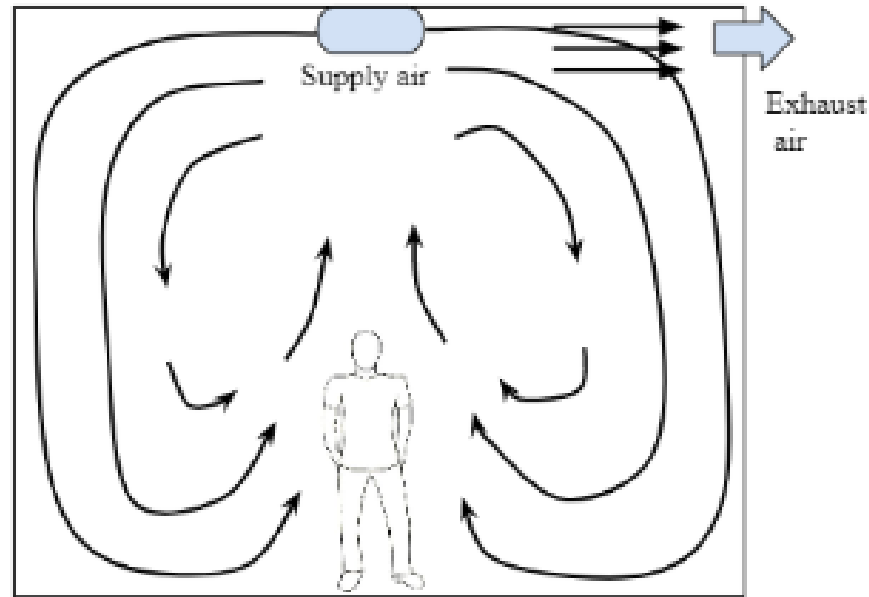

Figure 1: Schematic of a mixing-ventilation system

On the other hand, displacement ventilation systems supply air at low velocity near the floor level and mostly at lower temperatures than the room temperature. Buoyancy forces are used then to displace this air to higher levels where the contaminated air which is lighter will be extracted through openings in the ceiling. A DV system has the potential to provide the goal of achieving nearly good air quality in the breathing zone as the supply air. However, the flow pattern of this flow might be contaminated and changed when it comes in contact with materials, users of the room or heat sources. Figure 2 shows the air movement of a room with a heat source(person) in the middle.[3]
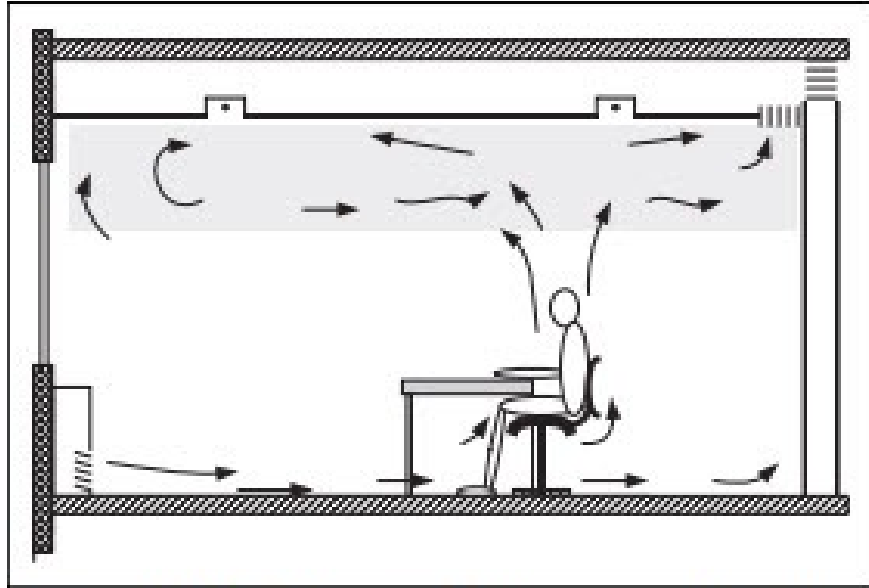
Figure 2: A schematic of DV system with a heat source

Common applications of displacement ventilation includes;

- Theaters, halls and casinos where the amount of contamination is high due to the number of contaminants.

- Schools, offices, restaurants etc.

Diffusers can be floor-mounted,or wall-mounted for a DV system. Example of such a diffuser is the CBA wall mounted diffuser from Lindab [4] given below in Figure 3a shows a radial diffuser while Figure 3b shows a wall linear diffuser.[5]

(a) Wall-mounted diffuser

(b) Schematic showing the flow and V_{max} of the diffuser above

2.3   Indoor Air Quality

Air quality is a very significant issue when talking about ventilation inside a building. Supplying a room with a clean air is one of the important tasks that environmental engineers must deal with. Air quality can definitively affect the indoor climate of a certain room or a building. A polluted air is the cause of many health problems due to the gases, chemical components and particles contained in it. There are many ventilation systems that provide solutions for that kind of engineering tasks, amongst them is displacement ventilation which is further studied in this work.

2.4   Air distribution in displacement ventilated rooms

The difference of density between the air supply and the air in the room will cause the air with the highest density to drop and the one with the lowest to be on top. The air will divide itself in thermally stratified layers. Thermal Stratification is the key of achieving a good air quality in displacement ventilated room. Amongst the factors that will cause a mixing of the stratified air, are moving people or door opening and closing it will cause higher air velocities as well. Displacement ventilation can also be utilized as a supply method that to achieve both thermal comfort and ideal air quality.

2.5 Displacement ventilation zones

These zones of DV can be classifies into the following;

   I Establishment zone.

  II Acceleration zone.

 III Gravitations zone

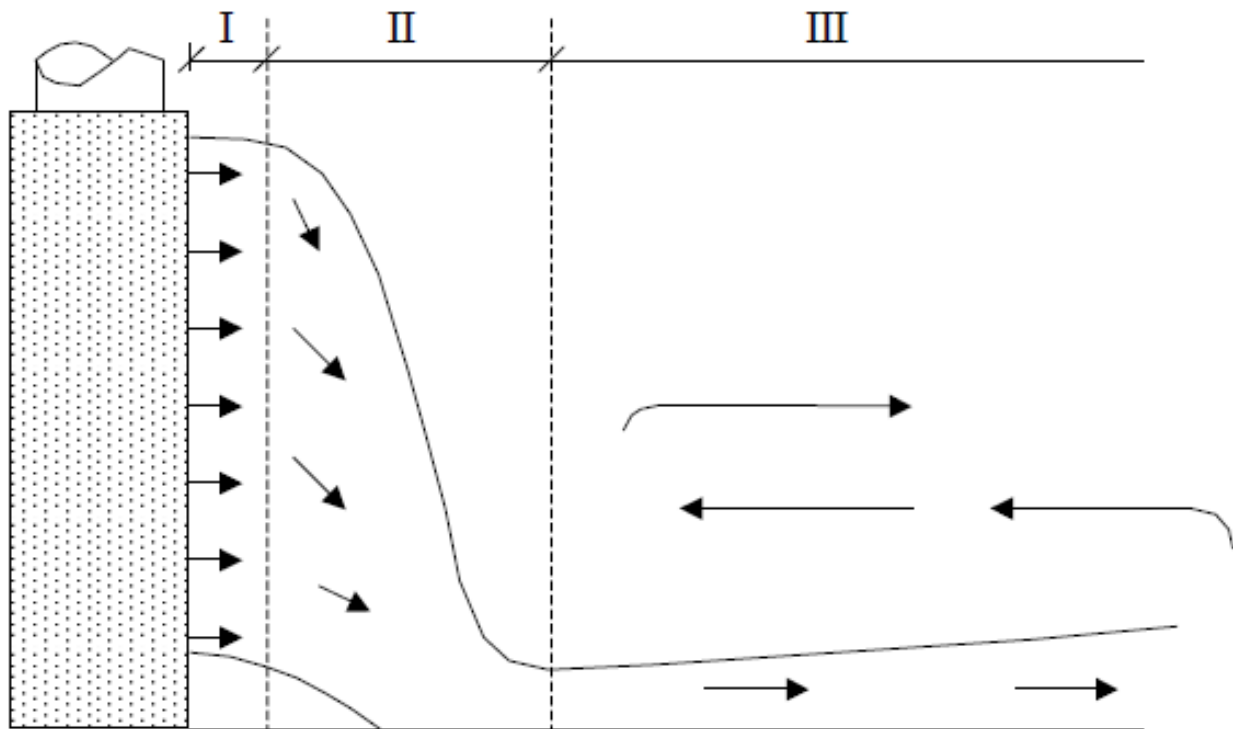The figure below shows the sketch of such a system. [6]

Figure 4: Acceleration region and Velocity decay region

The velocity of the establishment zone is dependent on the design of the diffuser.
The acceleration and gravitations zones are of great importance to engineers since it is within these two regions that maximum velocity as well as the occupant zone are found.

- Acceleration region. The air velocity becomes higher than the supply velocity at some distance from the supply unit due to difference in temperature between the supplied air and room temperature. The flow then drops downwards towards the floor thus increasing the velocity of the supplied air. This will

7

in turn lead to decrease in the thickness of the jet. The supplied air then spreads towards the floor and forms a jet-like flow. Since this air is cooler than the room temperature and higher velocity than the supply area, there is a risk of draft at horizontal distances from the supplied air. To avoid this, the occupant zone should not be in the area adjacent to the supply unit. The occupant zone is also where there are many different types of contaminants. The thermal plumes of the heat source (people and other heat producing sources e.g computers) changes a portion of the cool air from the diffuser thus reducing the velocity of the supplied air from reaching intended distances in the room and causing stagnant zones. Vertical movement is also caused by contaminants thus creating vertical movement of the supplied air which in turn risks being exhausted by the outlet unit. There is also the risk that the supplied air only pushes the contaminant air even further towards the ceiling. The result of this might be less low air with low temperature and velocity reaching all intended areas in the room.

- Velocity decay region The gravitational phase (also referred to as secondary zone) is the occupied zone where as the name suggests there is a decrease in the velocity in the x-direction. The velocity of the flow jet is important in this region since the occupants of this zone will not be comfortable due to draft. The supply temperature's velocity decreases while increasing its temperature due to warmer temperature from the floor and the ascending contaminated air. The final phase is also the occupancy zone where the walls and any blockage to this horizontal flowing direction of the supply jet will change the characteristics and direction.

2.6 Characteristics of DV

Basic characteristics of most DV include;

- Convective currents. This occurs as a two layer flow where the air that is being displaced stratifies in the upper zone.[8] The convection heat flow is the result of the fluid and solid interface. The heat transfer rate increases because of the bulk flow of the fluid. This explains why the rate of heat transfer through fluid is higher by convection than conduction.

- Thermal stratification. Layers of stratified zones develop due to the rise of temperature from the cold supply jet on the floor towards the upper zone. Heat sources create these thermal plumes thus driving the contaminant concentration and temperatures upwards. Improvement of air quality in the occupied zone is thereby achieved.

- Gravity currents. These are thermally driven air currents that occurs when cool air currents flows along the floor in DV. Contaminants and obstacles help these currents be redistributed throughout the room. In warm gravity currents, warm air moves from the warm spaces towards the cooler areas.

2.7 Convective plume over a person:

To be able to predict the air flow pattern in a room one must calculate the velocity and air flow over a person. Air flow rate is generated due to the convective heat from the person or a particular heat source. Convective heat varies with the activity level, clothing, and temperature. These factors will give differences when estimating the convective plumes. The height at where people are sitting is also an important factor when calculating the convective plumes. The generated airflow will be higher at a given point over the floor since the plume has more time to develop and drag air from the room.

2.8 Buoyancy force

The buoyancy phenomena occurs, when the lighter warm air is being pushed upwards because of the vertical gravitation forces. The same situation is faced in DV, where the cool supply-air coming from the inlet will displaces the air from the room in an upwards movement towards the ceiling. The supply-air will than become warmer due to the temperature rise. This fluid will thus continue loosing density due to the reduced gravity.

2.9 Literature review of computing near-zone velocity models

A literature review was carried out from different models that have carried out experiments in order to get overview of the conditions and characteristics of the near-zone. The scope of these tests have been the need to evaluate the length of the decaying zone as well as the velocity near the floor. These include :

- Nielsen's model
  This model is regarded as the most widely used model of computing near-zone velocity models.[10] The model uses an experimentally determined constant K_{dr}. The air speed decay in the secondary zone for a wall diffuse with a radial distribution can be found using;[11]

$$\frac{v_x}{v_f} = k_{dr}\frac{H_{diff}}{x} \tag{1}$$

where

- v_x is the maximum horizontal speed at a distance x from the diffuser [m/s]

- v_f is the face velocity of the diffuser [m/s]

- K_{dr} is the experimentally determined constant independent of x [-]

- H_{diff} is the height of the all mounted diffuser [m].

- x is distance from the diffuser

The setback is that k_{dr} is valid only for a specific diffuser with a specific size and specific supply conditions thus need for laboratory measurements for each diffuser with its specific conditions. This is uneconomical and time consuming.

- Nordtest model

Nordtest is an outcome of the research project undertaken by the Norwegian Building Research Institute [SINTEF Byggforsk] in order to validate the semi-empirical equations for designing displacement ventilation proposed by Prof.em Eimund Skåret. These equations will be discussed later in this paper. Nordtest is based on mathematical methods that use co-efficients that are independent of supply conditions and diffuser size. The experiments undertaken by SINTEF Byggforsk are valid for diffusers under non-isothermal conditions.

The maximum velocity in the acceleration zone near the diffuser is calculated by 2

$$V_{max} \approx k_{1,max} \cdot Ar^{k_{2,max}} \cdot B \tag{2}$$

$k_{1,max}$ and $k_{2,max}$ are two coefficients found in laboratory measurements.

Ar is the dimensionless simplified Archimedes number proposed in Nordtest methods [7]

$$Ar = \begin{cases} \frac{g'L^5}{q_t^2} & \text{for radial ATDs} \\ \frac{g'L^2}{q_t^2} & \text{for linear ATDs} \end{cases} \tag{3}$$

Where:

- $g\prime$ = reduced gravity [m^3/s]

- L = horizontal perimeter of diffuser [m]

- q_t = Total air volume flow rate [m^3/s

Buoyancy flux has been given as;

$$B = \left(\frac{q_t \cdot g'}{L} \right)^{\frac{1}{3}} \tag{4}$$

where the reduced gravity g' is given by;

$$g' = \left(9.81 \frac{\Delta \theta_t}{\theta_r} \right) \tag{5}$$

θ_r is in Kelvin

$\Delta \theta_t$ is the difference between the reference temperature and inlet temperature.

3 Method

3.1 Computational Fluid Dynamics

Fluid (liquid and gas) flow analysis are governed by partial differential equations that represent the conservation of mass, momentum and energy. Computational fluid dynamics(CFD) is the use of applied numerical mathematics methods, algorithms and physics by means of computer-based simulations to analyze fluid flow, heat transfer and associated phenomena. Knowledge of these equations is therefore critical before computing a CFD simulation. A good CFD simulation is one whereby the results can be analyzed and interpreted.

3.2 The governing equations

CFD is based on the Navier-Stokes equations. The governing equations will be given in this subsection. The conservation law of physics states that :

- Mass is always conserved and cannot be created or destroyed. This is also referred to as Continuity Equation. Since we are using incompressible Newtonian fluids, the density ρ is constant and the mass conservation takes the form

$$\frac{\partial u}{\partial x} + \frac{\partial v}{\partial y} + \frac{\partial w}{\partial z} = 0 \tag{6}$$

This equation is for a three-dimensional mass conservation at a given point and shows mass is always preserved for the fluid.

- Newton's second law states that the rate of change of momentum is always equal to the sum of the forces on a particle. This is also written simply as

$$F = m \cdot a \qquad\qquad [N] \qquad\qquad (7)$$

where F is the total forces involved while 'm' is for mass and 'a' is for acceleration.

- Momentum equation

  This equation is based on Newton's second law. The two forces that act on the a fluid particle are;

  – Body forces that include gravity.

  – surface forces i.e Viscous and pressure forces

  momentum on the x-direction can be written as[12]:

$$\frac{\partial(\rho u)}{\partial t} + \operatorname{div}(\rho u \mathbf{u}) = -\frac{\partial p}{\partial x} + \operatorname{div}(\mu \operatorname{grad} u) + S_{Mx} \qquad\qquad (8)$$

ρ is the density

  momentum on the y-direction can be written as:

$$\frac{\partial(\rho u)}{\partial t} + \operatorname{div}(\rho v \mathbf{u}) = -\frac{\partial p}{\partial y} + \operatorname{div}(\mu \operatorname{grad} v) + S_{My} \qquad\qquad (9)$$

  momentum on the z-direction can be written as:

$$\frac{\partial(\rho w)}{\partial t} + \operatorname{div}(\rho w \mathbf{u}) = -\frac{\partial p}{\partial z} + \operatorname{div}(\mu \operatorname{grad} w) + S_{Mz} \qquad\qquad (10)$$

S_M is the source momentum in the direction.

- The energy equation is based on the first law of thermodynamics, and is required when studying compressible flow. It can be written as:

$$\delta q + \delta w = de \qquad\qquad (11)$$

where δq and δw represent an incremental amount of heat and work respectively, which are forms of

12

energy. When this is added to a system, the internal energy de changes. Through a control volume this can be directly translated into

$$\iiint\limits_{\mathcal{V}} \dot{q}\rho d\mathcal{V} + \dot{Q}_{\text{viscous}} - \iint\limits_{S} \rho \mathbf{V} \cdot \mathbf{dS} + \iiint\limits_{\mathcal{V}} \rho(\mathbf{f} \cdot \mathbf{V})d\mathcal{V} + \dot{W}_{\text{viscous}}$$
$$= \frac{\partial}{\partial t} \iiint\limits_{\mathcal{V}} \rho \left(e + \frac{V^2}{2} \right) d\mathcal{V} + \iint\limits_{S} \rho \left(e + \frac{V^2}{2} \right) \mathbf{V} \cdot \mathbf{dS} \tag{12}$$

and in the form of partial differential equations as

$$\frac{\partial}{\partial t} \left[\rho \left(e + \frac{V^2}{2} \right) \right] + \nabla \cdot \left[\rho \left(e + \frac{V^2}{2} \right) \mathbf{V} \right]$$
$$= \rho \dot{q} - \nabla \cdot (\rho \mathbf{V}) + \rho \left(\mathbf{f} \cdot \mathbf{V} \right) + \dot{Q}'_{\text{viscous}} + \dot{W}'_{\text{viscous}} \tag{13}$$

where $\dot{Q}'_{\text{viscous}}$ and $\dot{W}'_{\text{viscous}}$ represent the proper forms of the viscous terms

3.3 Turbulence models

Since the turbulence structure of a flow is dependent on the flow itself, we will look at what computational procedures and models that are used by the system.

Turbulence models are divided into two main models namely [12] ;

- Classical models which are based on time-averaged Reynolds equations. These models include:

    1. zero equation model

    2. two-equation model - $\kappa - \epsilon$ model

    3. Reynolds stress equation model

    4. algebraic stress model

- Large eddy simulation which are based in space-filtered equations.

Reynold-Averaged turbulence models in the CFD software Star CCM+ include;

1. K-ϵ Turbulence

    The different K-ϵ turbulence models being used in this study include:

    - The standard K-ϵ

        The standard K-ϵ turbulence model is based on two transport equations that solves the turbulent

13

kinetic energy and its dissipation rate ϵ. In addition to that, the model in STAR-CCM+ has been upgraded by adding to it features to account for effects such as buoyancy and compressibility. High y+ Wall Treatment is used in this turbulence model.

- The standard K-ϵ Low-Re

  This turbulence model is involving the low Reynolds number approach. Typical for this model is, that it provides more damping functions, which make it perfect to apply for the viscous-affected regions near walls. The use of this model is suitable for particular purposes such as natural convection problems. Possible to use All y + Wall Treatment and Low y+ Wall Treatment.

- AKN K-ϵ Low-Re

  Like the previews model, this model contains the low Reynolds number as well. However, the Reynolds number has different coefficients than the standard K-epsilon model, and uses different damping than the standard K-epsilon Low-Re model. This model is recommended where the flow is complex and the Reynolds number is low. Possible to use All y + Wall Treatment and Low y+ Wall Treatment.

- Realizable K-ϵ

  According to STAR-CCM+, this model is much better than the Standard K-epsilon model in many ways, and is a great option when it comes to getting as accurate as possible answers. Although, both the standard and realizable models are available in STAR-CCM+ with the option of using a two-layer approach, which enables them to be used with fine meshes that resolves the viscous sublayer.

- Realizable K-ϵ Two layer

  This model combines the Realizable K-ϵ using a Two-layer All y+ Wall Treatment approach.

2. K-Omega Turbulence

   This is also a two equation model where the turbulent kinetic flow, κ and the specific dissipation, ω equations governing the turbulence of the flow are solved. The two models for this turbulence model include;

   - SST(Menter) K-Omega

     This model has three wall options namely:

     - All y+ Wall Treatment,

- High y+ Wall Treatment,

- Low y+ Wall Treatment.

- Standard (Wilcox) K-Omega

  The wall options for this k-ω model are ;

  - All y+ Wall Treatment,

  - High y+ Wall Treatment,

  - Low y+ Wall Treatment.

3. Reynolds Stress Transport Turbulence

4. Spalart-Allmaras Turbulence

The k-ϵ and the k- Omega are models are used in this study.

3.4 The boussinesq approximation

Since we are trying to solve a displacement ventilation problem, which is a non-isothermal flow, the boussinesq approximation can be used to simplify the CFD simulation. This approximation doesn't solve the full equations of the Navier-Stokes, but simplifies it by having no variation of density in the flow field while giving rise to the buoyancy forces.

3.5 Radiation

In STAR-CCM+ there are two thermal radiation models available:

- Surface-to-Surface radiation modeling

- Participating Media Modeling

Surface-to-Surface radiation modeling considers only the radiating and absorbing surfaces and neglects the medium that fills the space between the surfaces. The Participating Media Modeling does not neglect the medium, which means that the medium can emit, absorb and scatter radiation.

3.6 CFD-modeling

CFD numerically solves equations of fluid flow, namely the equation of continuity, the energy equation, three momentum equations, a transport equation and low turbulence model equations for a fluid domain

with applied boundary and initial conditions. The utilization of CFD provides us with simulation that can be used to analyze among others temperature distributions, flow patterns and heat transfer in rooms by giving solutions in 2D or 3D, transient or steady state.

The CFD codes contain the following components:

- Pre-processor

- Solver

- Post-processor

Pre-processor

Pre-processing is the stage where the user inputs and defines the problem to be simulated and calculated by the software. The geometry was defined with input parameters from different guidelines for the three different simulations undertaken in this paper. The analysis in this paper have both been done by 3D and 2D. A Three-Dimensional mesh is first created before it is converted for simulations carried out by the 2D flows. The following were however common activity for the models;

- Defining the geometry with measurements.

- Creating a sketch of the geometry and any other domain needed.

- Creating a sketch extrusion of the sketch since models are created with a 3D tool .

- Creating geometry part.

- Separating and assigning boundary surfaces for the geometry part created by splitting by patch and assigning region for the geometry part.

- Generating a 3D grid which is sub-dividing the domain into small number of non-overlapping sub-domains. This is also referred to as mesh. Details of the meshing properties are given under the meshing section of each simulation.

- Defining the fluid properties which are given in different tables. Some of this might need to be calculated or assumed. Assumptions can lead to errors in the solutions. However some assumptions are not avoidable.

Solvers

The splitting of the domain into smaller sub-domains(mesh) are meant to allow the solvers to run the

governing equations inside each of these sub-domains. There are three main methods that these governing equations are discretized by the solvers. These are;

- Finite difference method.

- Finite Element method.

- Finite volume method.

The discretized governing equations solves the aspects of transport, mass, momentum which includes energy and continuity equations, convection and radiation .

Post processing

The user is able to analyze the solution both under simulation and after the simulation is finished. Solution can be visualized, recorded and monitored by creating reports and plotting relevant data. Tracking is also available using animations in the STAR CCM+ software. These results can thus be exported to other software programs that can interpret tabular data for example XY data for velocity within the domain. An example of such a software that has been used extensively in this paper is MATLAB developed by Math-Works.

3.7   CFD simulations vs. Experiments

Both CFD and experiments give quantitative prediction and analysis of flow systems. The former uses numerical algorithm to solve equations while the latter uses physical measurements. Using CFD saves time and resources in comparison in comparison with physical measurements and experiments. With CFD, one can simulate and analyze large scale models while experimental fluid studies are mostly defined to laboratory-scale models. The models in experimental fluid studies have limitations on the quantity of experiments performed while a CFD simulation can be repeated many times just by adjusting the model and its values. Experiments are also slow and single purposely intended while a CFD simulation is faster and multiple problems can be solved using the same simulation.

3.8 Limitations of CFD simulations

Limitations of CFD models include;

- uncertainty in the models and knowledge of the system to be simulated. This includes the numerical calculations that run in the background of the system which can be hard to understand if the user does not have enough competence of the same.

- Errors in data which can be due to;

  - Numerical errors which are introduced when an solving equations.

  - Truncation errors that arise from approximation in differential solvers.

  - Rounding off to sizes that are defined by the different computer setups and programs.

  - Values that are set in by the user. The computer system does not have a way of telling the user that these values are the correct values for that particular simulation.

- Physical errors. CFD solutions can only be accurate by how much the user is accurate in defining the physical model of the process.

- It is not possible to get the exact mesh to represent the real scenario of a room and the flow of air in the room.

- Boundary condition specifications where one has to choose which boundary condition provides the best domain for a particular simulation.

4 Validation

4.1 Comparison between CFD simulations and Benchmark (2D steady state case)

In this validation, a 2D steady state test case with the air as the working fluid is carried out. Different turbulence models were used with the purpose of comparing the results with existing experimental data. This validation takes the well known benchmark test [14] as a guideline and comparison report. The main objectives of this section is to simulate and compare the different turbulent models with experimental measurements that were performed earlier [13]. The convergence of the residual depends on the type of grid used. It takes longer to reach the convergence when using a fine mesh in comparison with a coarse mesh. On the other hand, the use of a coarse mesh leads to less accurate results. A finer mesh gives better results compared to experiment.
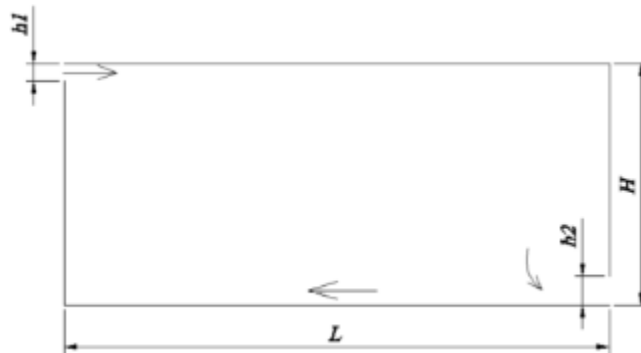
Figure 5: Sketch of model room

Figure 5 shows a sketch of the model room with the dimensions given in the benchmark test as:

- Length = 9 m

- Height = 3 m

- h_1 = 0.168 m

- h_2 = 0.48 m

The inlet is on the upper left corner while the outlet is at the right bottom corner. This is an example of a mixing ventilation system.

- V_0 = 0.455 [m/s]

- $k_0 = 1.5*(0.04u_0)^2 = 4.97 \times 10^{-4}$ J/kg (turbulent kinetic energy)

- $\epsilon_0 = \frac{k_0^{1.5}}{l_0} = 6.59 \times 10^{-4}$ J/kg (turbulent disputation)

Where the length scale is defined as:

- $l_0 = \frac{h_1}{10}$

4.2 Turbulence models

The following turbulent models were used in the different simulations;

4.2.1 Standard k-epsilon

The standard K-ϵ turbulence model is based on two transport equations that solves the turbulent kinetic energy and its dissipation rate. In addition to that, the model in STAR-CC+ accounts for effects of buoyancy and compressibility.

4.2.2 Standard k-epsilon Low-Re

This turbulence model is involving the low Reynolds number approach. Typical for this model is, that it provides more damping functions, which make it perfect to apply for the viscous-affected regions near walls. The use of this model is suitable for particular purposes such as natural convection problems.

4.2.3 AKN K-epsilon Low-Re

The Abe-Kondoh-Nagno K-epsilon Low Reynolds number model is unlike the Standard K-epsilon model, because thy both have their own coefficients. The two models are using different damping functions that reduce the turbulent viscosity. The damping functions are mathematical functions that progressively reduce the value of the turbulence viscosity to zero at the wall. AKN K-epsilon Low-Re is known to work well for complex flows, and is a good choice where the Reynolds numbers are low but the flow is relatively complex.

4.2.4 Realizable K-epsilon

The epsilon (ϵ) stand for the new transport equation for the turbulent dissipation rate. The equation lets the model satisfy certain mathematical constraint on the normal stresses consistent with the physics of turbulence (realizability). This model is substantially better than the Standard K-Epsilon model for many applications, and can generally be relied upon to give answers that are at least as accurate.

4.3 Measurement points
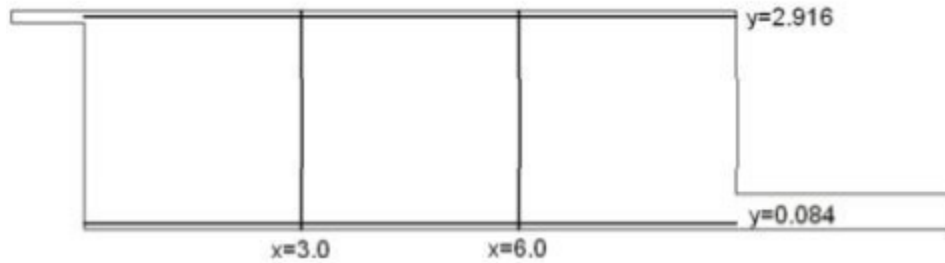
Figure 6: Sketch of the vertical and horizontal lines where the velocity profiles have been measured

After running the simulations in STAR CCM+, data was imported from the XY-plots (velocity-values of the given positions from benchmark) to be plot in MatLab with the objective of analyzing the effect of mesh and turbulence models on velocity of the supplied fluid. The velocity is normalized by dividing it by 0.445[m/s]. Figure 6 shows the positions of the vertical and horizontal lines that data was retrieved from. At x = 3 and x = 6 we could find out how the vertical velocity profile varies. The comparison of velocity between simulations and measurements shows the similarity between the chosen model and the measurement. On the other hand, the horizontal velocity profile have been measured near to the ceiling at y = 2.916 and near to the floor at y = 0.084.

4.4 Mesh

The accuracy of the simulation and its convergence can depend on mesh refinement. The number of the cells and the nodes at the inlet and the outlet have a big impact on the convergence. The following meshing models were chosen:

1. Surface Remesher

   By choosing the surface remesher the quality of the mesh-surface as well as the volume mesh will be well formed. The surface remesher will form the surface into triangles repairing the current mesh. The surface remesher targets the edges and makes the mesh finer in this area of the model. Other parts such as localized refinement that are based on part surfaces or boundaries can also be included. The correction of the volume mesh is among the conditions to be taking to consideration. For that reason the selecting of the surface remesher is necessary and critical for the whole simulation in general.

2. Trimmed Cell Mesher which generates cubic control- volume shapes. This mesh type also uses less computational memory than the polyhedral.

3. Prism Layer Mesher

The layer of the prismatic cells used with a core volume mesh next to the wall surfaces or boundaries is of immense importance and it plays a critical role in getting an acceptable flow solution.

A prism layer option consists of four essential elements:

- Its thickness : Describes the Prism Layer Total Thickness properties. The prism layer thickness controls the total overall thickness of all the prism layers. When selecting the prism layer thickness node, the absolute or a relative size is accessible.

- Prism layer controls number of cell layers that are generated within the prism layer on a part surface or boundary.

- The size distribution of the layers controls the method that is used to calculate the thickness distribution of multiple cell layers within the prism layer.

- The function that is used to generate the distribution : The stretching function determines the underlying formula that is used to generate the cell layer thickness distribution.

Different base sizes was used to achieve different coarseness of the mesh. Table 1and Figures 7, 8, and 9 show the different mesh types. The choice for using trimmer cell mesher instead of polyhedral was due to the fact that trimmer cell meshing uses less memory. The Number of Prism Layers was = 5 for all of the meshes. At the inlet and the outlet and all over the edges the mesh is much more denser and finer, that will optimize the velocity profile and help providing a reasonable simulation.

Table 1: Base size and the number of cells

Mesh number	Base size	Number of cells
1	0.2m	12300
2	0.4m	4798
3	0.1	34763
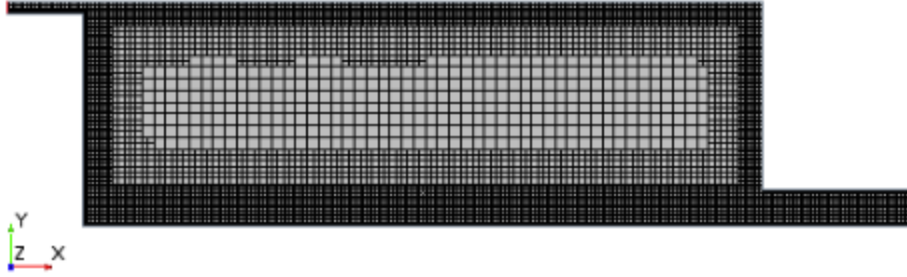
Figure 7: Mesh 1: reference Mesh
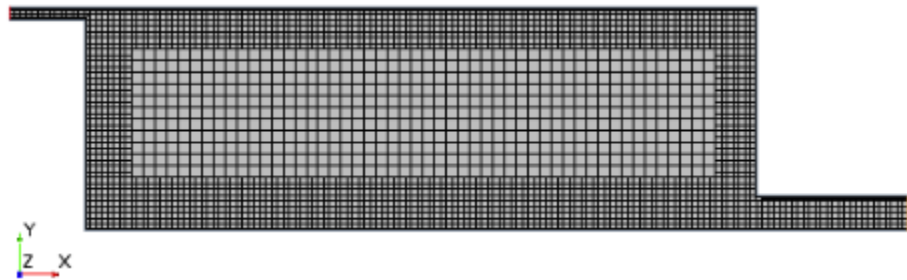
Figure 8: Mesh 2: coarse
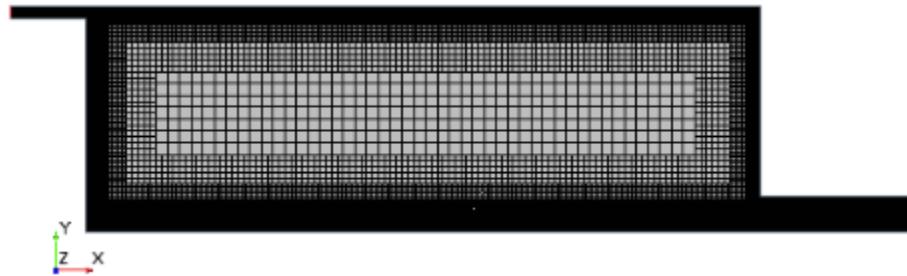
Figure 9: Mesh 3: fine

4.5 Residuals

Residuals is a tool used in analyzing the convergence (or divergence) of a simulation. When the residuals decreases, it means that they are depending on the details of the simulation that have been selected before running it, and equations that are run by the solvers.

4.5.1 Mesh-Residuals

Figures 10, 11, and 12 are representing the convergence of the two different meshes that have been selected, in addition to the reference one. One can observe, that with a finer mesh, the convergence is longer to reach.
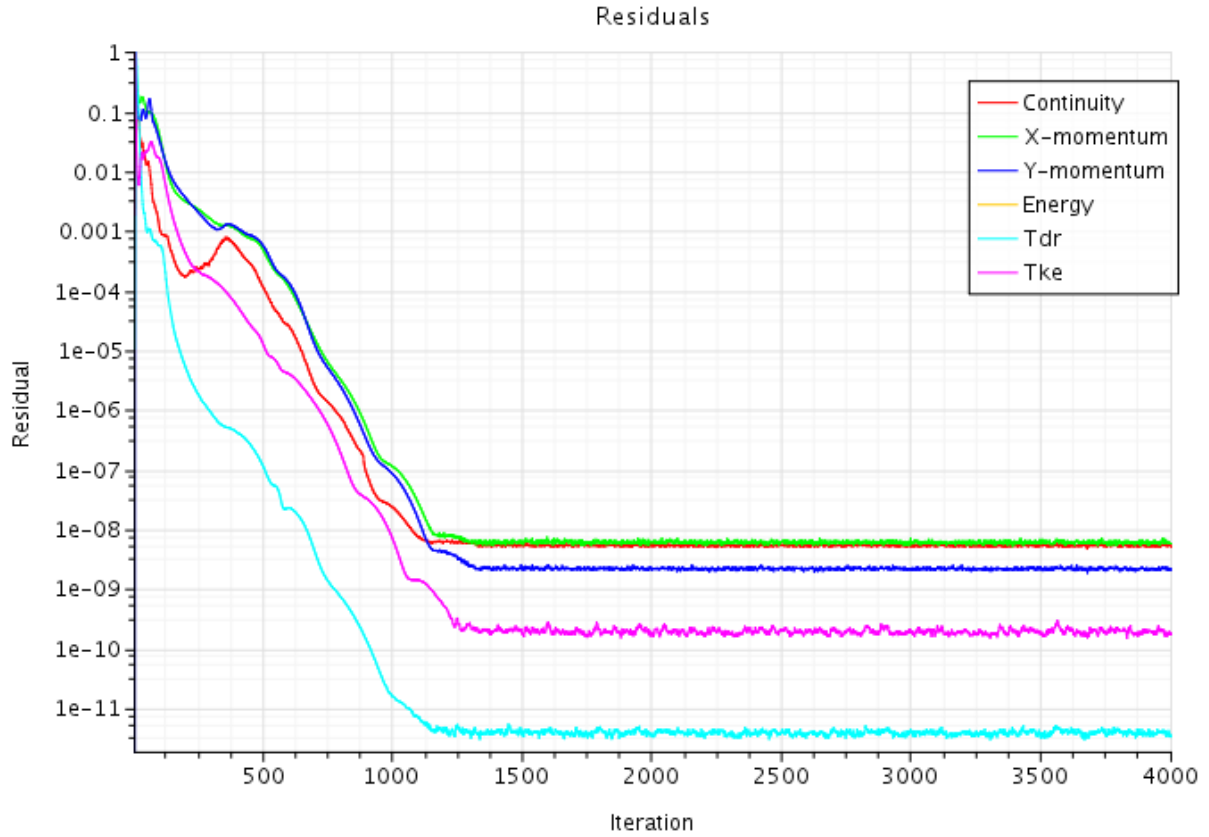
Figure 10: Mesh-coarse 2D
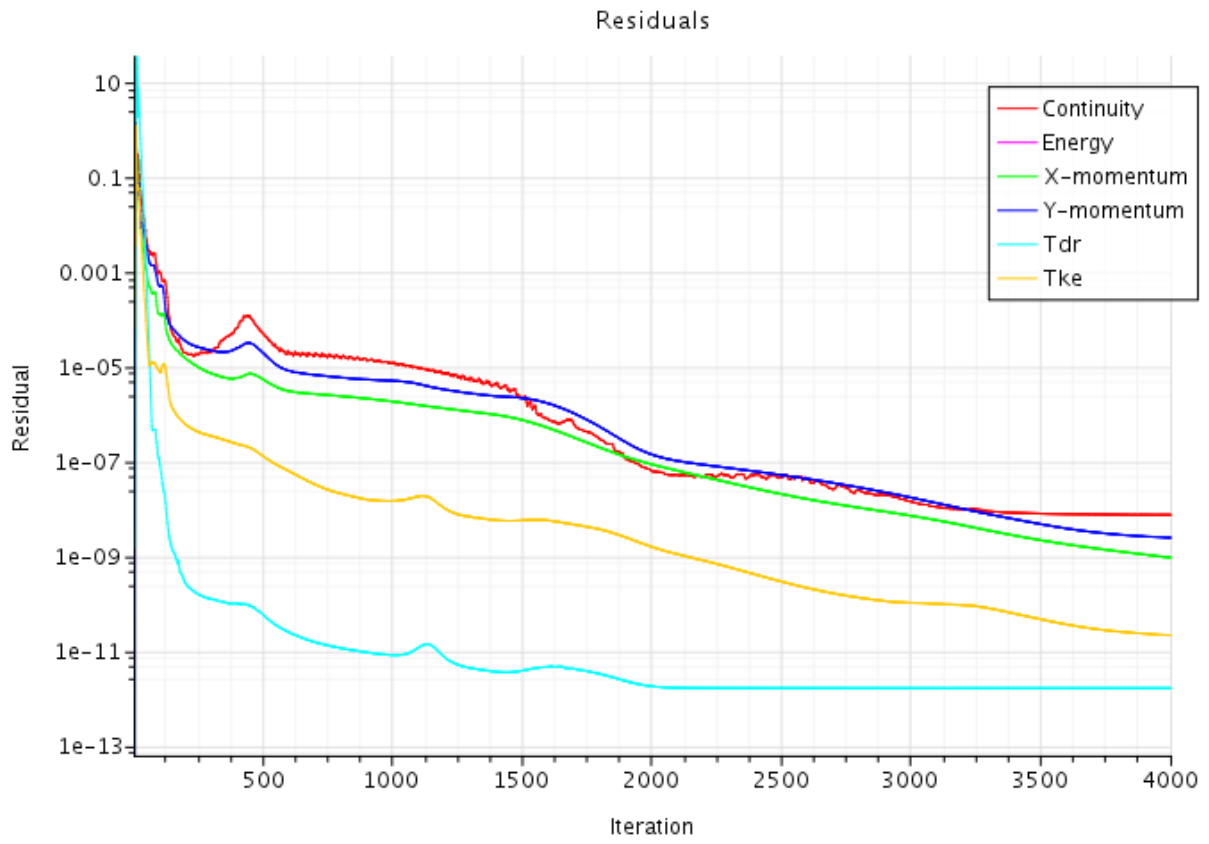
Figure 11: Mesh-fine 2D
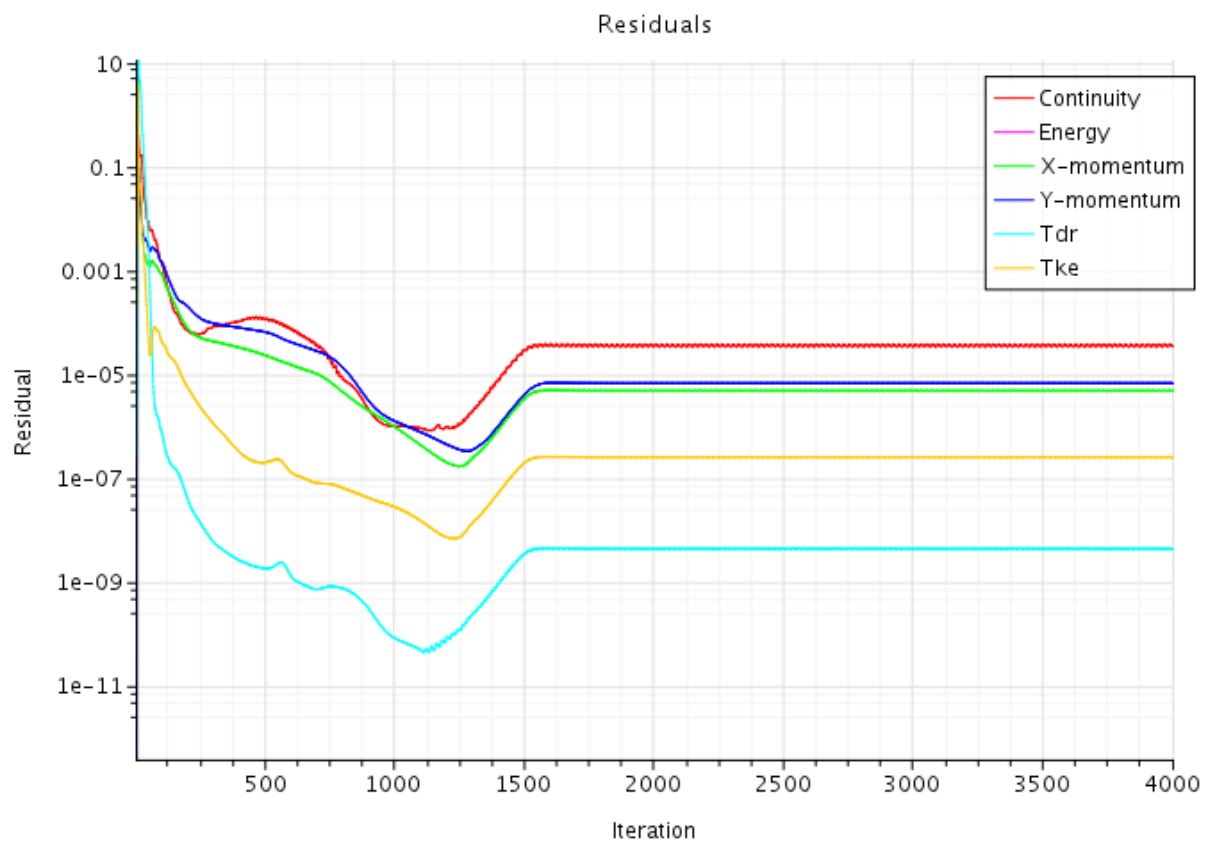
Figure 12: Mesh-reference (benchmark) 2D

4.5.2 Convergence of simulations different turbulence models

Figures 13-16, are showing the convergence of four different models that has been selected in STAR CCM+. Thy all show acceptable convergence that give reliable results.
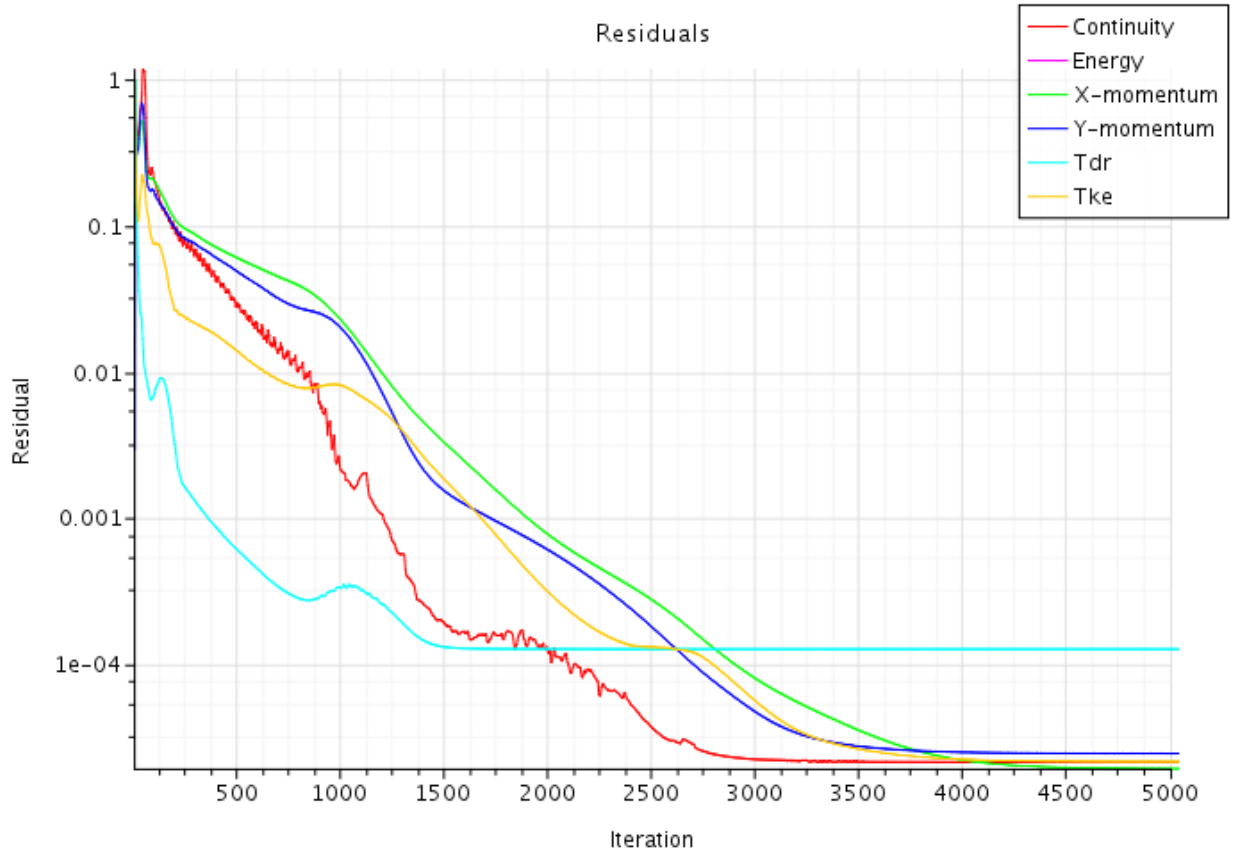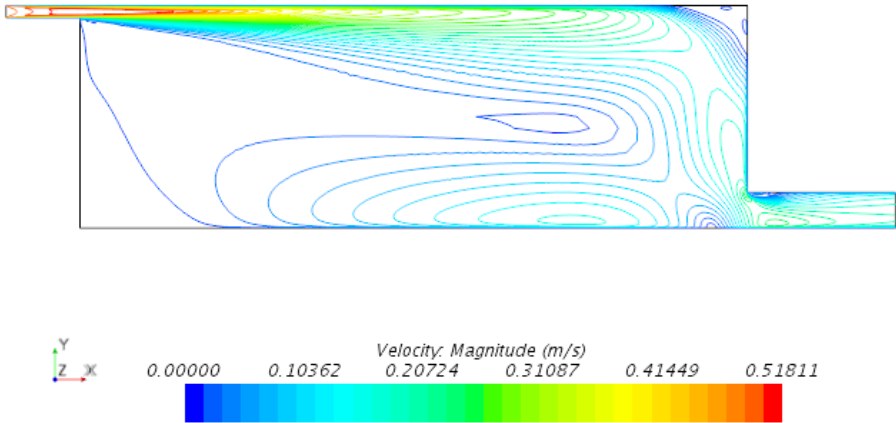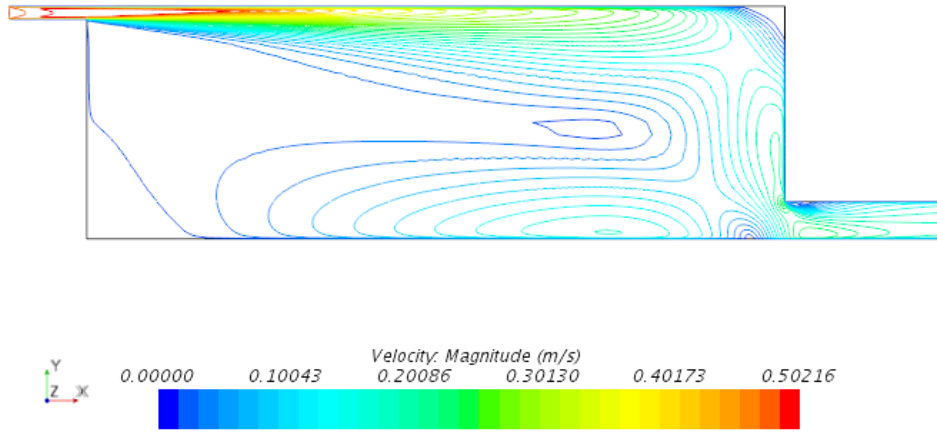

Figure 13: Simulation 3 Standard K $-$ ϵ
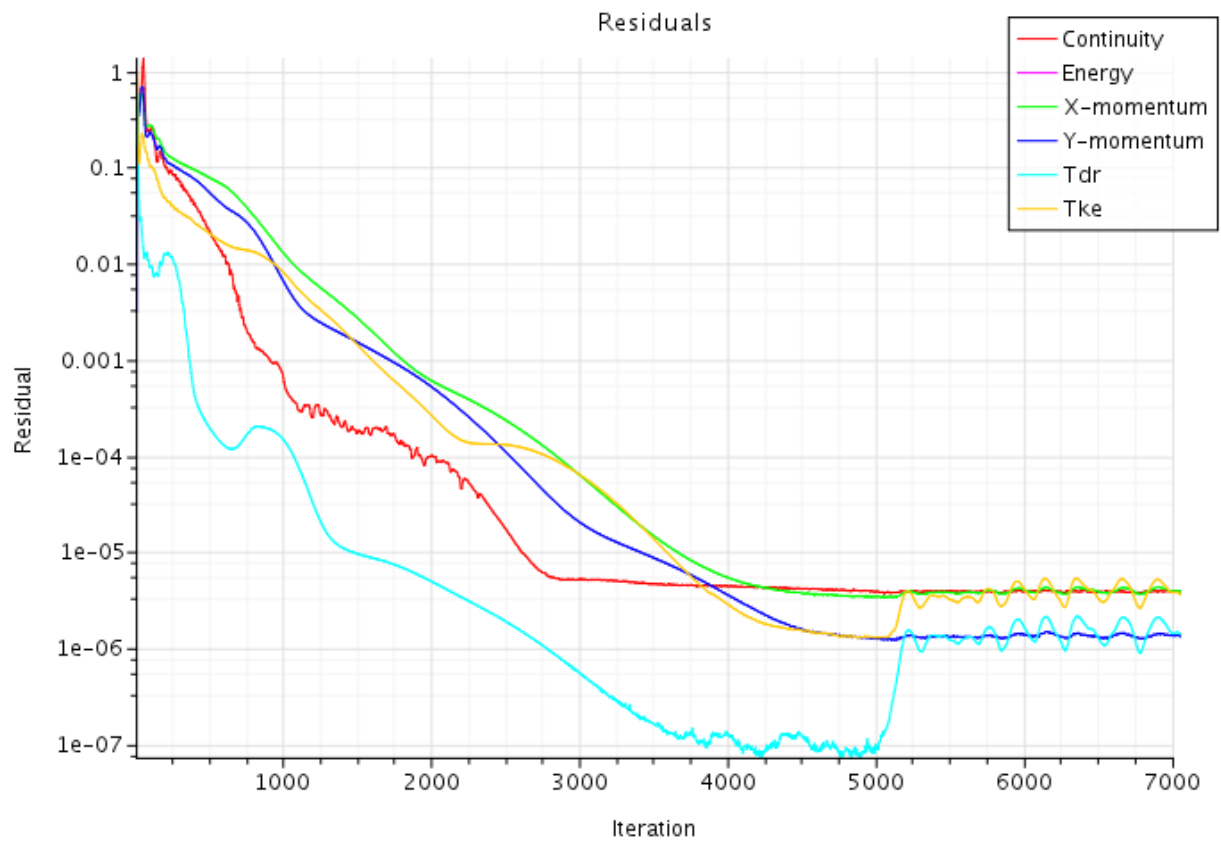
Figure 14: Simulation 4 Standard K – ϵ Low-Re
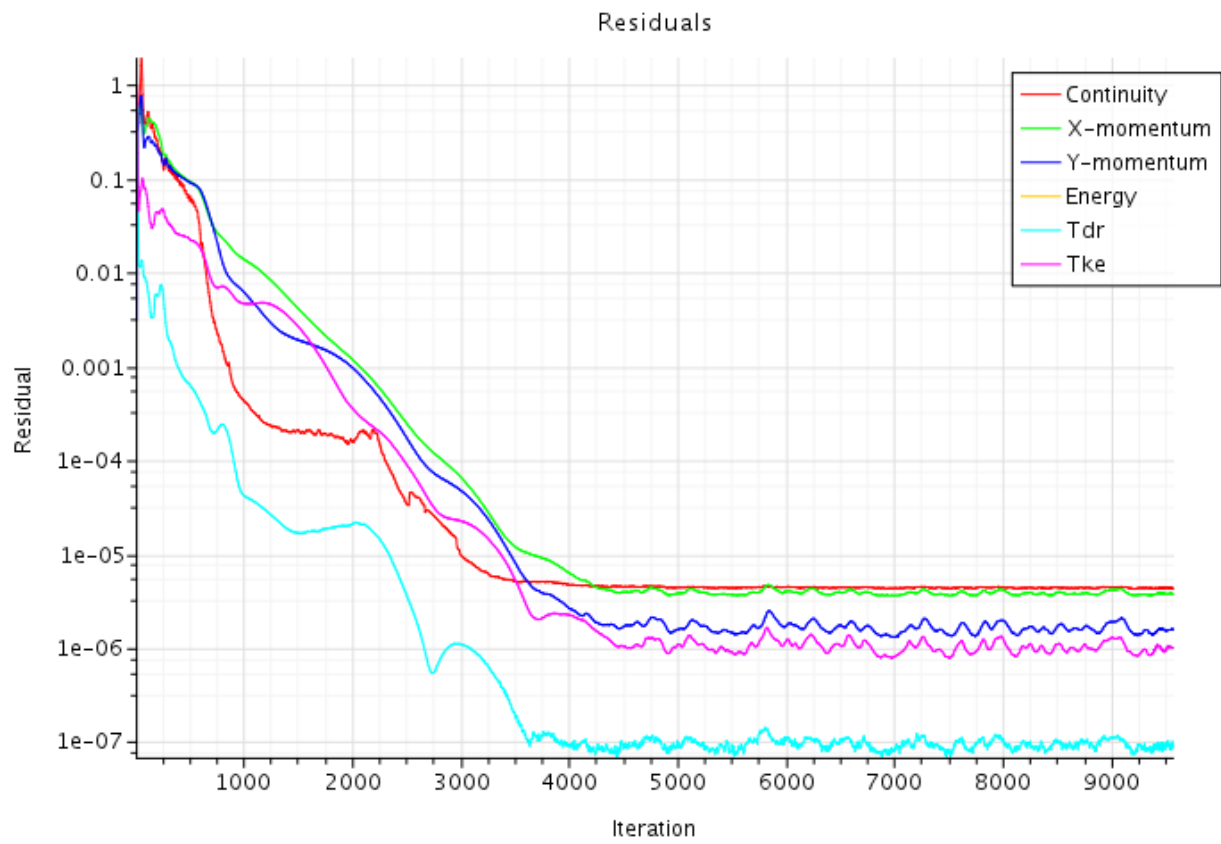
Figure 15: Simulation 5 AKN K $-\epsilon$ Low-Re
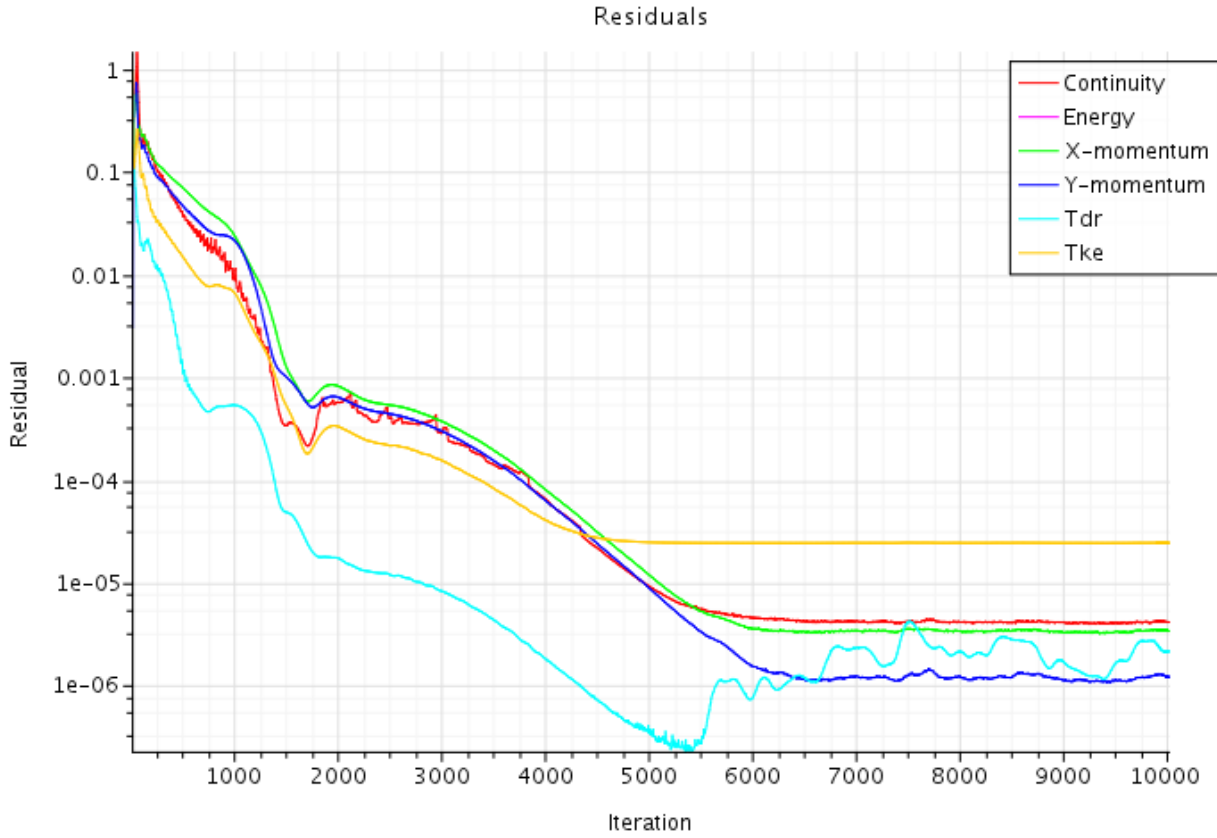
Figure 16: Simulation 6 Realizable K $-$ ϵ

4.6   Contour showing different turbulent models:

As mentioned before, the simulation which were made using the STAR-CCM+ showed approximations that almost match the result from the experimental data coming from benchmark. This can be confirmed by the observation of the figures that were results of the different simulations using the software. The following figures (17 to 20) are illustrations of scalar-scenes using four different turbulence models. All of them are showing velocity profiles that has been normalized by 0.455 m/s. the most common characteristic trait that they all share, is the big eddy in the middle right corner. The velocity of the supply air coming from the diffuser represents a jet-flow that has the highest value near the inlet where the acceleration region is. It is difficult to notice the difference between all the four turbulence models. All the four models give an acceptable approximation to the existing experimental data, but some differences are still there to observe. The jet flow from the inlet cannot move along the ceiling so far as in the AKN K-epsilon Low Re. What remarkable

about the Realizable K-epsilon model is, that the flow is more turbulent due to the air-fluctuations that occur on the left side of the test room. The thickness of the jet flow on the Realizable K-epsilon model is much larger compared with the other models, and the acceleration region is much shorter. However, all of the models that are represented in this subsection are showing the drop of the supplied air when hitting the wall except the realizable K-epsilon model where the air drops much earlier. The characteristics of the air velocity behave quite different from all of the rest of the models in the realizable k-epsilon.

Figure 17: Simulation 3 standard $K - \epsilon$

Figure 18: Simulation 4 standard K − ε Low-Re
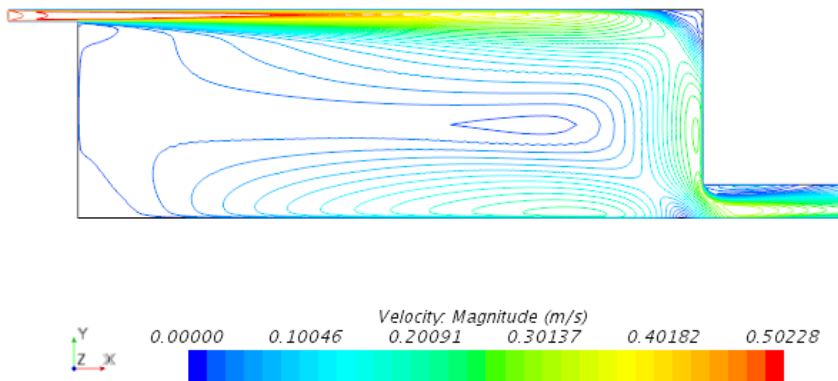
Figure 19: Simulation 5 AKN K − ε Low-Re
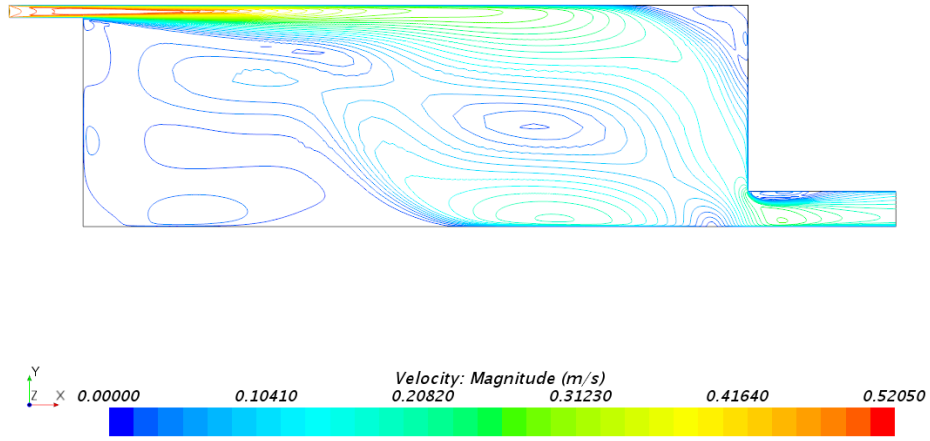
Figure 20: Simulation 6 Realizable K $-$ ϵ

4.7 MatLab plots

4.7.1 Velocity profiles of different meshes vs measurements
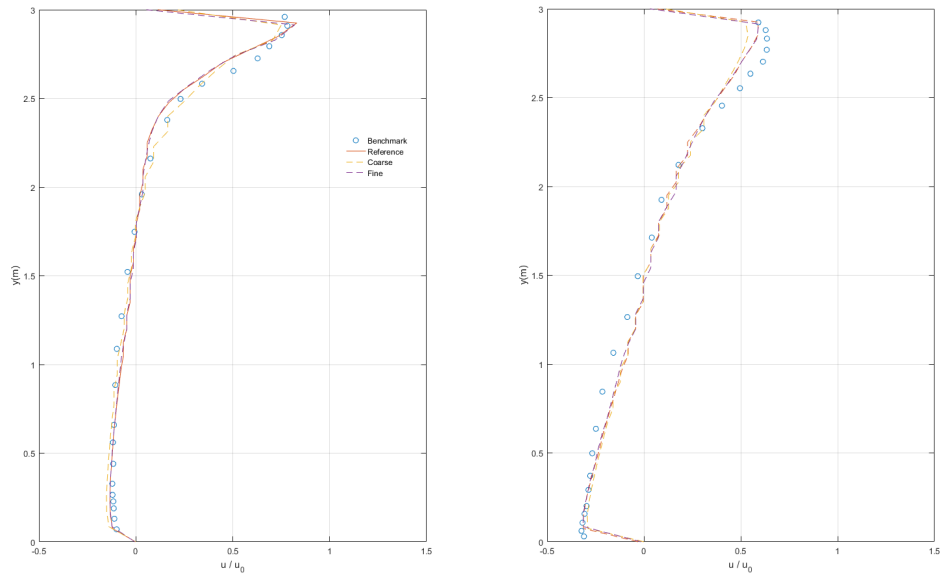
(a) vertical velocity profiles with different meshes at x=3

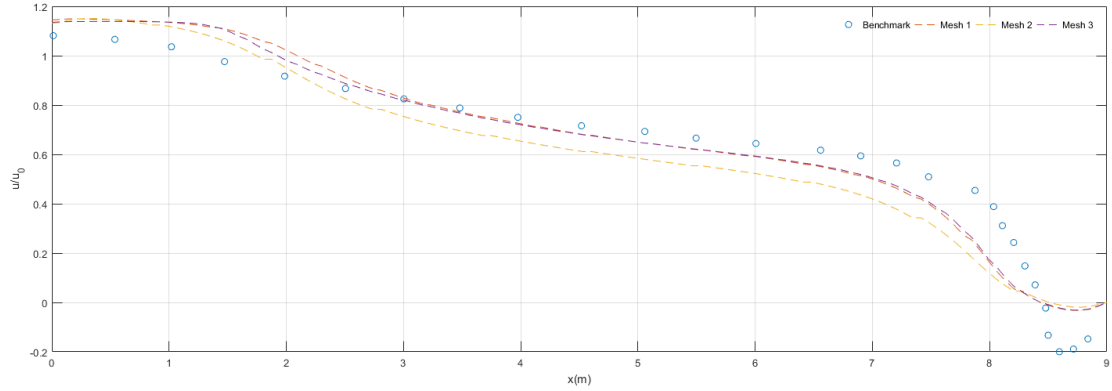(b) Vertical velocity profiles with different meshes at x=6

Figure 21

33

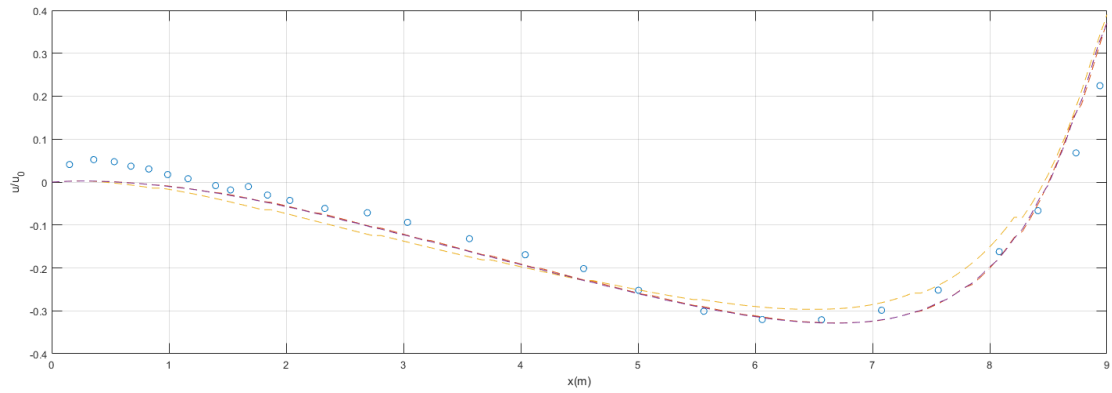Figure 22: The horizontal- top velocity profiles for different meshes vs measurements

Figure 23: The horizontal- bottom velocity profiles for different meshes vs measurements

After getting the results from the MatLab plots, one could observe that some of the CFD-simulations did almost overlap the measurements from benchmark.

The mesh resolution is extremely important as this determines whether the solution is realistic. Simulations with three different meshes were conducted with the purpose of comparing them to experimental data from benchmark. This made it able to run the grid-independence test. The main purpose of this work is to investigate which mesh that not necessary needs to be refined to match up with the one from the benchmark. It turned out that mesh 1 and mesh 3 overlap each-other, which is illustrated in all of the velocity profiles (Figures: 212223) for the three meshes.

As a result of the experiment, one can conclude that mesh 1 is in good agreement with the measurements.

4.7.2 Velocity profiles four different turbulent models vs measurements

x

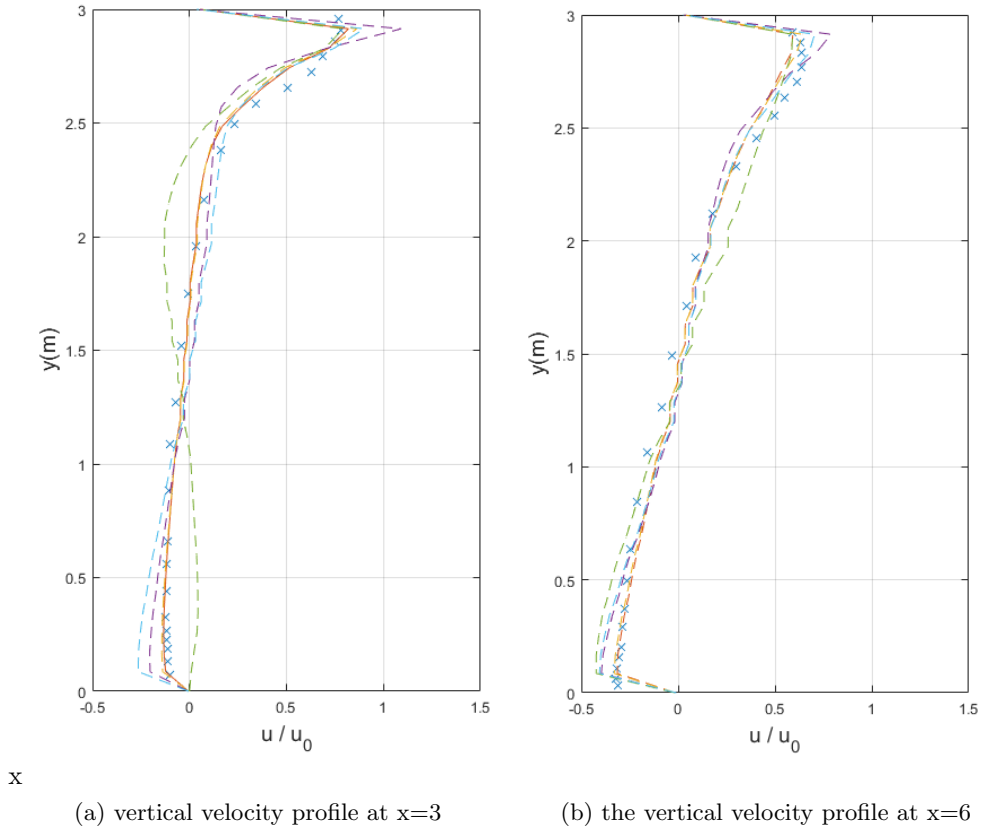(a) vertical velocity profile at x=3   (b) the vertical velocity profile at x=6

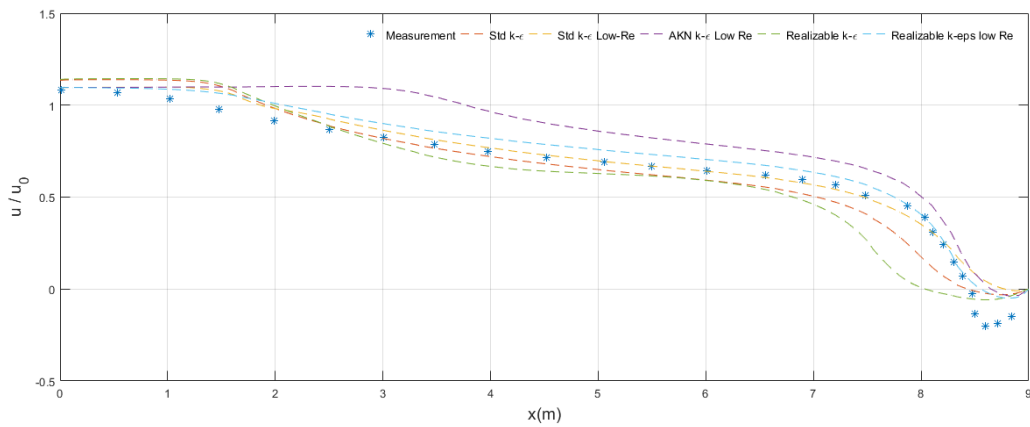Figure 24: the vertical velocity profiles of the four turbulent models compared to benchmark

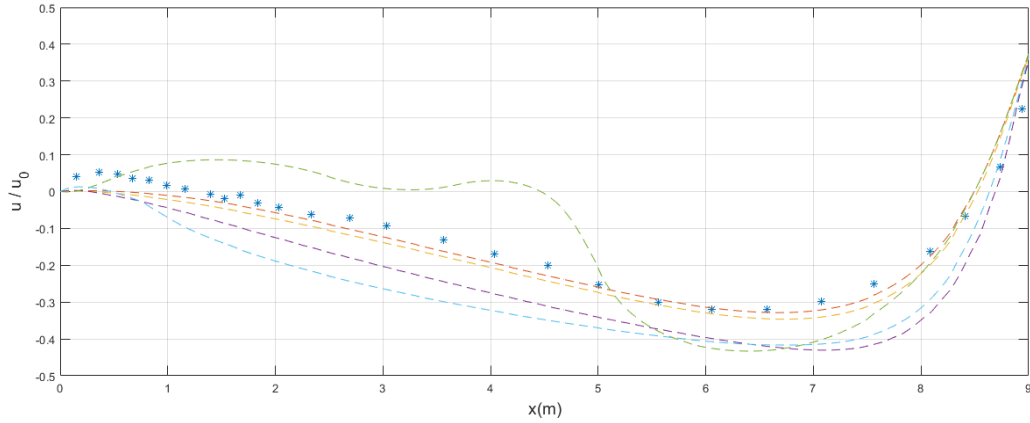Figure 25: The horizontal-top velocity profile vs benchmark

Figure 26: The horizontal-bottom velocity profile vs benchmark

Figure 24a and b represents vertical velocity profiles with the five turbulence models vs experimental data. Vertical line-probes was taken at x = 3 m and at x = 6 m following the benchmark model, while the height is equal to 3 meters which represents the y-axis. The first thing that catch the intension, is that the velocity near to the floor and the roof, is very low which explains the nonslip-condition phenomena. The velocity is at its highest V_{max} on the upper part of the room, and this is valid for both at x = 3 m and at x = 6 m. Horizontal line-probes (horizontal line locations) at the bottom at y = 0.084 m (see Figure26), and the top at y = 2.916 m (see Figure 25), were selected for the objective of comparing the turbulence models with the experimental data from the benchmark model.

4.8 Why benchmark?

Benchmark is one of the most reliable sources that has a good scientific investigation concerning this issue. All of the simulations were in 2D which made the work less time-consuming in comparison with the 3D simulations. Another reason that made us choose the benchmark model was the opportunity to compare the measurements with results from this study.

4.9 Conclusion

According to the results, the standard $k - \epsilon$ and the standard $k - \epsilon$ Low-Re appear to have similar trend. When analyzing the flow distribution throughout the given test-room, it turns out that all turbulence models give relatively similar flow patterns in the main stream away from the wall. All the five selected models are in good agreement with the result as benchmark results, except the velocity profile of the realizable $k - \epsilon$.

This can be due to the calculations in the background or other components not within our competence. However, we can conclude this section by stating that the results from this 2D study are comparable and in agreement with the measurements.

5 Three-Dimensional Study of DV

Tasks were set to conduct simulations with a DV case. Experimental data conducted by Lars Davidson [16] were then compared to this study of 3D DV simulations done in STAR CCM+. The task was to get better knowledge of ventilation in a three-dimensional room with a heat source, using the information to extend our knowledge on thermal-induced flows.

The results of this section of the study is compared to results arrived by Davidson. Furthermore, the results are also compared to results of measurements found in the journal. The published form of the study where these measurements were retrieved from is not available to us. To overcome this issue, a software called plot digitizer has been used to convert the scanned copy of the plots with the measurement results into a digital plot which was used to compare with results found in this section.

5.1 Model setup

The room is cubical with side length (L) = 0.5 m. The height of the inlet is 0.1 m and the heat source is found in the middle of the room ($0.48<x/L<0.52$, $0.48<y/L<0.52$, $0<z/L<0.22$).

The model is a 3D box simulation carried out using Star CCM+ with water as the working fluid.

The following boundary conditions were used for the turbulent model:

- $C_\mu = 0.09$

- $C_1\epsilon = 1.44$

- $C_2\epsilon = 1.9$

- $\sigma_k = 1.0$

- $\sigma_\epsilon = 1.2$

- $\sigma_t = 0.9$

The Boussineq model was used together with gravity. The realizable K-epsilon Two Layer model which a RANS model turbulent model has been used for these simulations. Two different simulations were carried out namely; Case Q200 and Case Q600. The Case Q200 is a steady state simulation while the Case Q600 is an unsteady simulation. Results were taken for the first 15 minutes (Maximum physical time $\tau = 900$ seconds) for the unsteady simulation and compared with the results by Davidson and the measurements.

38

A presentation of the mesh is given (see Figure 27) below showing the inlet (situated of the left size of the figure close to the floor) and the outlet (colored green and situated on the opposite size just below the top). The heat source is the extruding object centered in the middle of the floor.

The mesh is refined with volumetric controls near the heat source. The numbers 1, 2 and 3 represent the inlet, outlet and the heat source respectively.
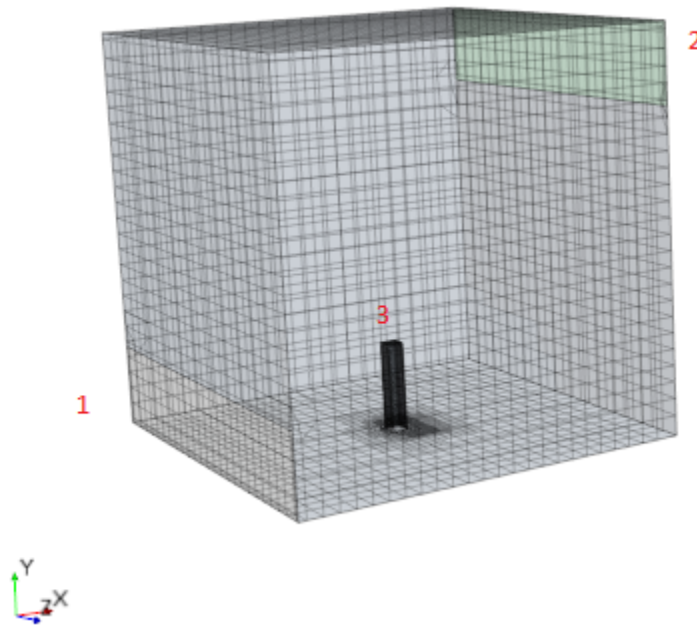

Figure 27: Mesh showing the inlet, outlet and heat source placement

The models chosen for the mesh are prism-layer mesher, surface remesher and trimmer. Base size for mesh is set to 2.0 cm. The resulting volumetric mesh has thus 37207 cells.

5.2 Initial conditions

The fluid is supplied from the inlet at a temperature of $13°$ (t_{in}) at a height of 0.1 m extending throughout the length of the axis. The initial temperature of the room has been set to $15°$ for both simulations. The heat source for the model has thermal specification as heat source with a power supply of 200 W (Case Q200) and 600 W (Case Q600).

The flow of a fluid is dependent on how free the flow path is from obstacles. It is expected that a DV system should have a jet-like flow near the surface of the floor due to the lower temperature and lower velocity of the supply air. A change of direction of the flow arises when the flow comes in contact with contaminants, for example a heat source which may include human and other heat producing objects. This phenomena is also true in this simulation since there is a heat source situated at the middle of the room. The location of the heat source and the small dimensions of the test room are reasons to why the flow does not follow a jet-like flow near the floor on the positive x-axis.

The fluid properties of these models are for water with the the following values.

- Specific heat 4182.72 J/kg-k

- Thermal conductivity of 0.62027 W/m-k

- Thermal Prandtl value of 0.9

5.3   Results and discussion

Boundary condition for the inlet is a mass flow inlet with a calculated mass flow of;

$$\dot{m} = \rho v A [kg/s] \tag{14}$$

where $\dot{m}$ is the mass flow rate = 0.1385 kg/s

v = inlet velocity = 0.00277 [m/s]

A = Areal of inlet = 0.05 m^2

No radiation is used in these cases since the temperature difference is not high. The dimensions of the domain is also a small compared to a real size room. Radiation has also been omitted since all walls, roof and floor have boundary specifications for thermal conductivity set as adiabatic. Davidson has given the reason for omitting the heat radiation as an acceptable approximation with water as the medium and that radiation does not affect the flow pattern significantly [16].

Thermal plumes are created near the heat source due to the upward movement of the flow while stratified zone can be clearly seen from the figures below. The following measurement points were used to check the temperature profiles (see Figure 28).

- point 1 x/L = 0.1 z/L = 0.1

- point 2 x/L = 0.9 z/L = 0.1

- point 3 x/L = 0.9 z/L = 0.9

- point 4 x/L = 0.1 z/L = 0.9

For both cases, layers of stratified flow are also formed. At the four given points above, the vertical temperature difference of approximately 1-1.5°C from the inlet temperature. This has been presented by normalizing the temperatures and defining temperature as t-t_{in}. The z-axis has also normalized and non-dimensional and hereby defined as z/L.

5.3.1   Case Q200

Figure 29a and 29b shows the thermal plumes of the flow and velocity profile. The vertical movement of the flow is also clearly seen in this figure. We observe a back-flow at the outlet and this might be due to temperature difference with the outside of the outlet. However, a field function temperature defined as t_{out} was created in order to reduce the impact of interference from outside conditions at the outflow. This temperature is a function of temperature inside the domain.
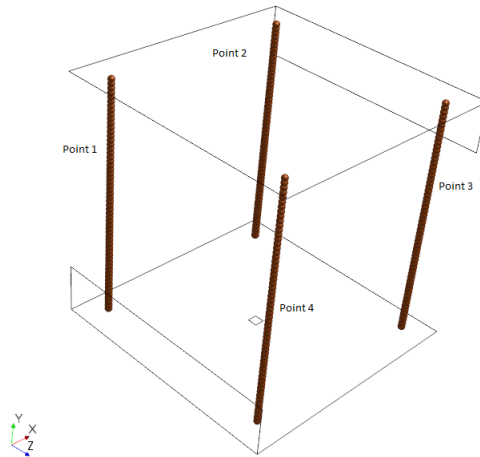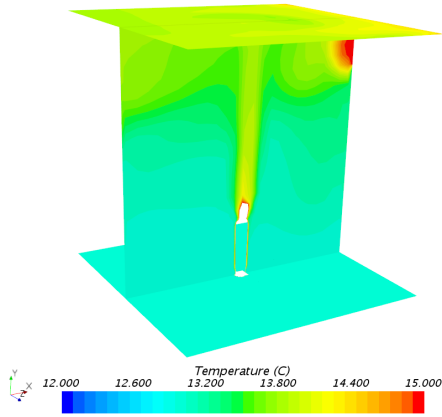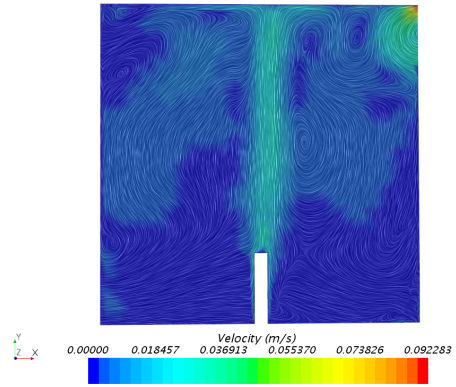

Figure 28: Measurement points

(a) Q200 steady state model

(b) Q200 Velocity profile.

Figure 29: Q200 Temperature and Velocity profiles

Figure 30 shows the temperature profiles for the four different vertical lines given in Figure 28 compared with measurement points from the digitized plot and results by Davidson. The plot is in good agreement with the results and measurement being compared against.
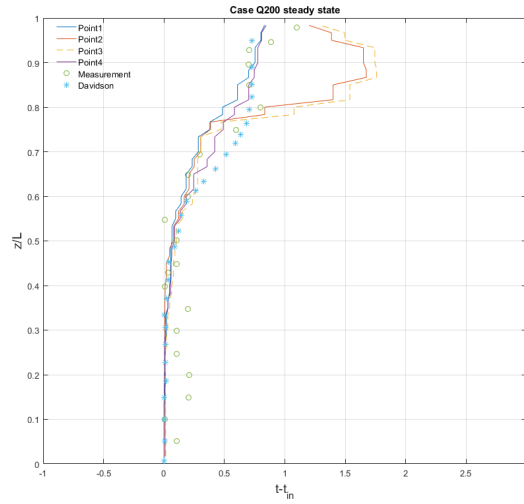

Figure 30: Case Q200

5.3.2 Case Q600

Case Q600 simulation run using the unsteady state solution has a heat source giving out 600 W. Case Q600 has a similar geometrical setup as the Q200 case. The results showed an approximate similar representation of the results arrived at by Davidson. A back-flow is also present in this model. The general system behind a displacement setup using an unsteady run was nevertheless observed despite of this issue. The temperature profile for this unsteady run is represented by Figure 31a while the velocity profile and vertical airflow pattern is represented by Figure 31b.
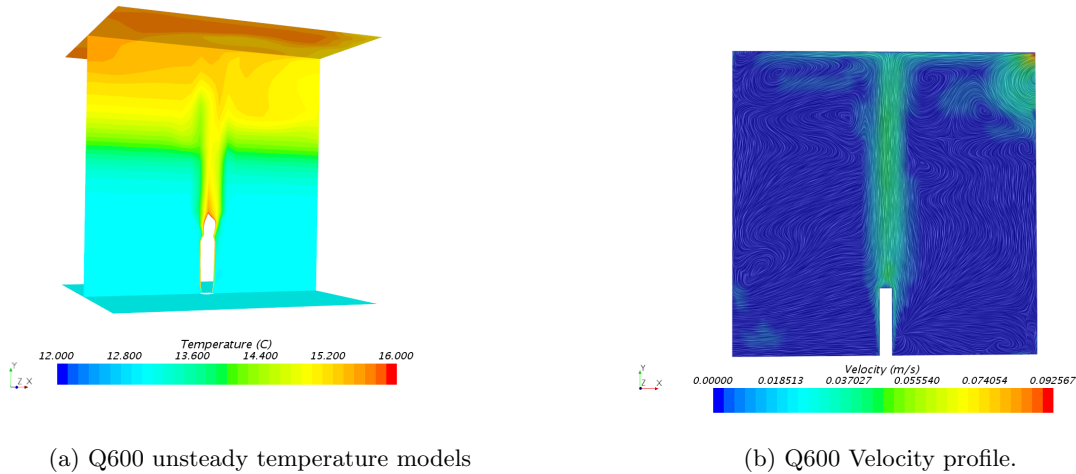

(a) Q600 unsteady temperature models

(b) Q600 Velocity profile.

Figure 31: Q600 Temperature and velocity profiles

The temperature profile for point 2 (see Figure28) (x/L = 0.9, z/L = 0.1) which is close to the outlet is measured and represented in the Figure 32 below. This result from the XY plot are then transferred to MatLab and a plot is generated. This plot is similar to the one given by Davidson at time = 900 seconds for both measurements and results obtained. The difference between any vertical point at the lower level and at the higher level of the same point is around 2°C which is similar to the values by Davidson.

Generally, the model show how the supply air and the contaminant air distribute themselves in separate zones (see Figure31a). The temperature in the lower zone is cooler than the upper zone which is what is expected from a DV system. The lower zone displaces the warm air towards the ceiling.
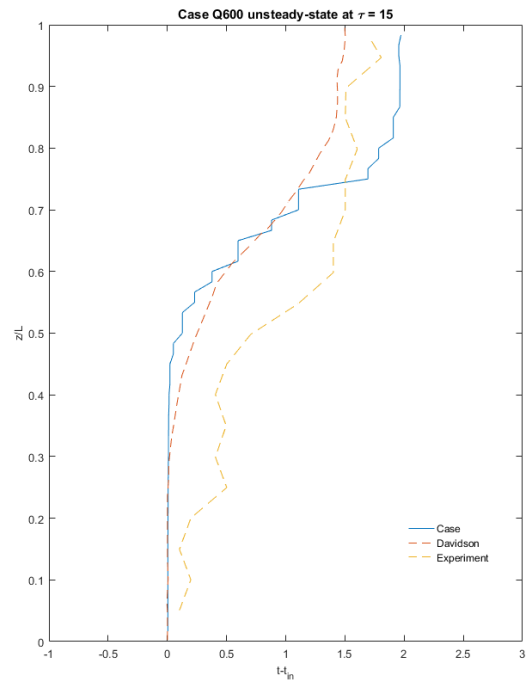
Figure 32: Vertical temperature profile at τ=15

6 Effect of diffuser height on 3D DV system

This chapter presents the results of the main objective of this study, which is to determine what effect the height of a diffuser has on the Archimedes number proposed in the Nordtest method NT VVS 083 [7]. Skåret proposed that the Archimedes number for both radial and linear diffusers is independent of the diffuser height, we have therefore conducted various simulations where the height of the diffuser, the inlet flow rate and the heat load changes.
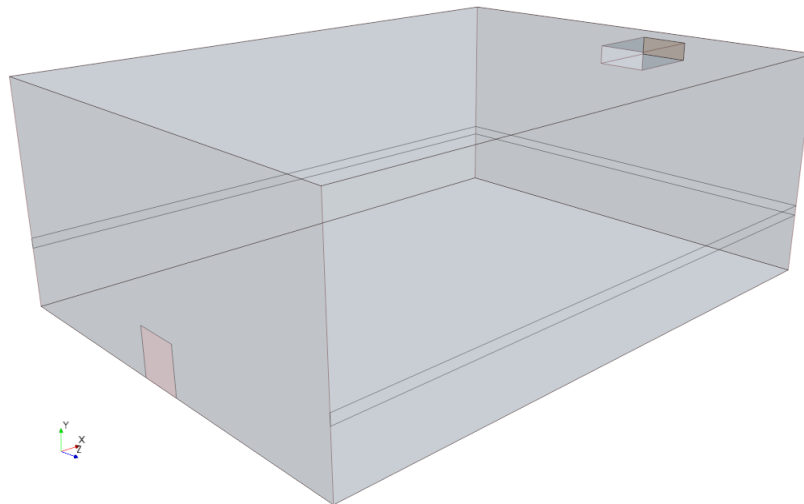
6.1 Model setup

Figure 33: Geometry

This study strictly follows the guideline of the Nordtest method. The CFD model is based on a standard room with dimensions suggested in the Nordtest method, shown in figure 33. The dimensions are 7.5 m (length) by 5.6 m (width) by 2.8 m (height). A linear wall mounted displacement ventilation (DV) diffuser centered on the wall is installed at floor level with dimensions summarized in table 2. The supply velocity profile is very constant over the entire supply area. The air leaves the room on the opposite wall of the diffuser with the dimensions 0.70 m by 0.25 m and a length of 1 m. Heating is provided by cables attached to the walls at a height of 0.75 m above the floor. The applied heat loads for different cases are summarized in Table 2.

6.1.1 Mesh generation

The mesh was generated by doing an automated mesh under operations in the geometry node. The surface remesher, trimmed cell mesher and prism layer mesher were selected to execute the mesh. Based on our previous experience, mesh refinement is done near the inlet and the bottom section of the room. This is done by a volumetric control with a block part under parts in the geometry node. The mesh was generated with 4 prism layers and a thickness of 0.03 m. The generated mesh had a total number of 548,541 cells.
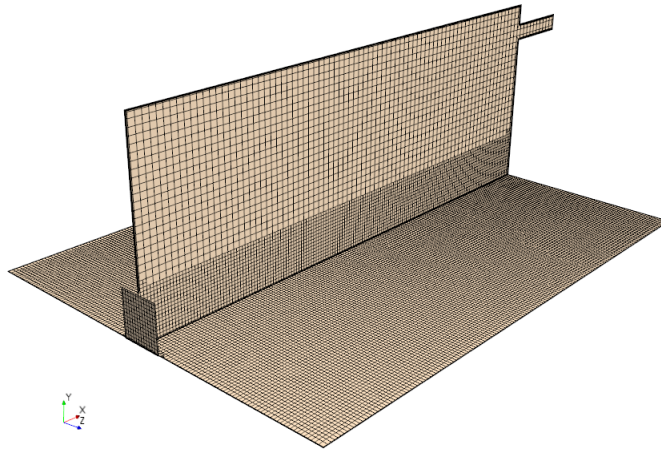

Figure 34: Mesh at plane section z/H = 1

6.1.2 Physics

In STAR-CCM+, all the simulations have been steady state runs with a gas type region for the room air. The flow is coupled flow, and the equation of state is constant density to be able to use the boussinesq model with gravity. The viscous regime is turbulent and the $K - \omega$ turbulence model standard $K - \omega$ (Wilcox) was used combined with the All y+ Wall Treatment. This turbulent model has shown to perform well in these kind of studies [18]. Radiation has also been taken into account in these simulations to get a more realistic environment. The surface-to-surface radiation model was chosen with gray thermal radiation as radiation spectrum. This also enables the view factor calculator.
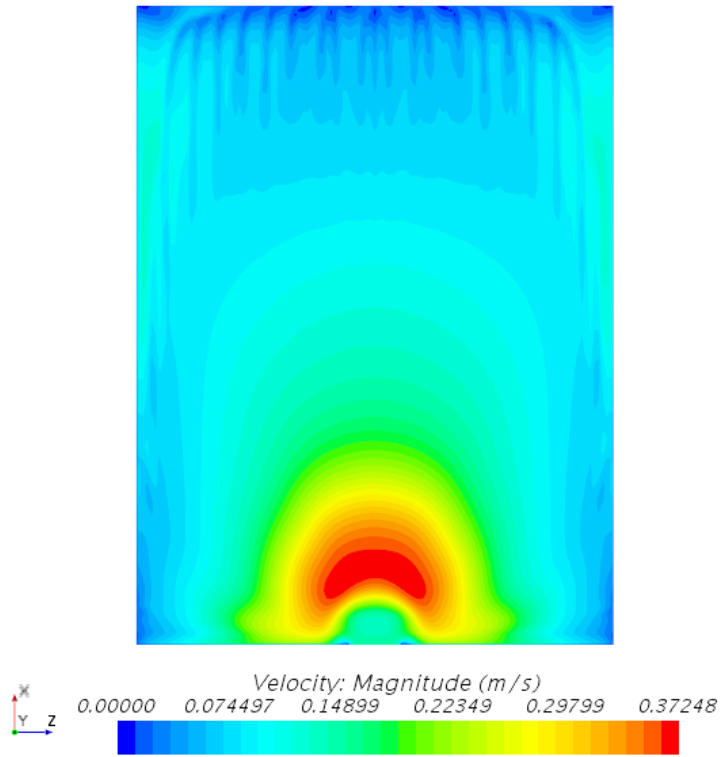
6.1.3 Boundary conditions

We have used 0.36 W/m^{2}K as U-value of all vertical walls, floor and roof. The temperatures of all surfaces were set to 24°C and the initial temperature was set to 24°C. In STAR-CCM+ the volumetric flow of the inlet boundary condition had to be converted to mass flow, this is done by using density of air (1.216 kg/m^3) at 17°C and applied at the inlet boundaries. The surface emissivity, surface reflectivity and surface transmissivity were remained at default, 0.8, 0.2 and 0 respectively.
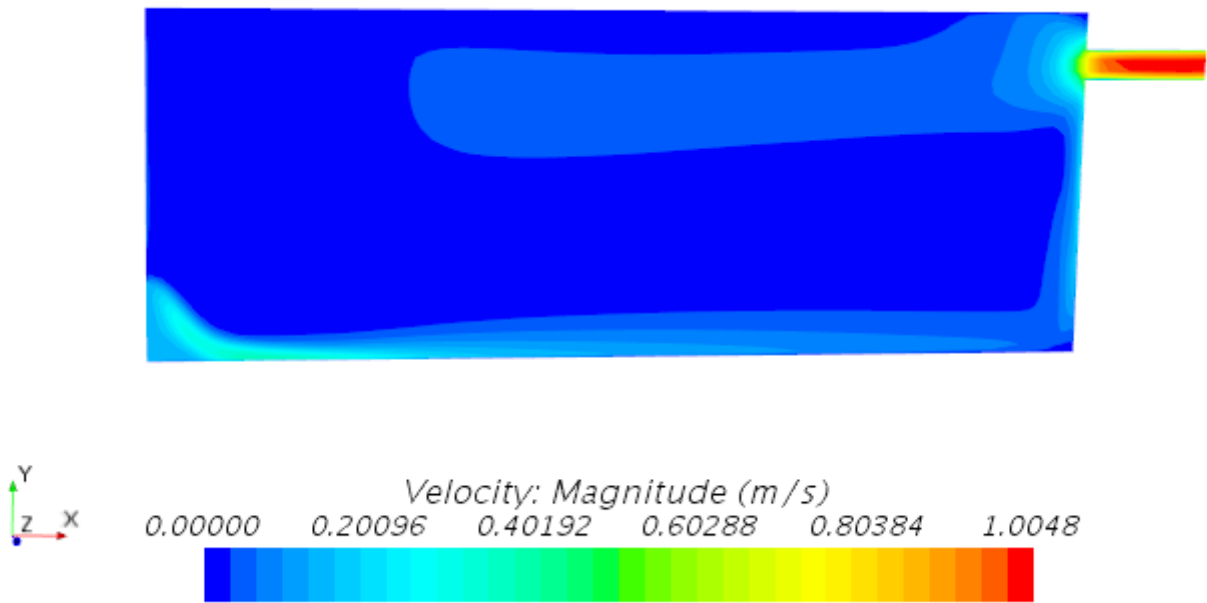
6.2 Results and discussion

Extracting the results for the max velocity profile was done by making vertical line probes at z/H = 1 in STAR-CCM+. The first line probe is 0.1 from the diffuser. From 0.1 m to 0.9 m the distance between the line probes are at 0.1 m. From 0.9 to 7.2 m the distance between the line probes are at 0.3 m, making it a total of 30 vertical line probes. The data where then exported to MatLab to find maximum velocity for each distance from the diffuser. Extracting the results for the temperature profiles was done by making vertical line probes at 1 m from the diffuser and 5 m from the diffuser. They were both at z/H = 1.

Based on the Nordtest NT VVS 083 method, the reference temperature is an average of at least five measurements of the air temperature at a height of 1.1 m from the floor and at a minimum distance of 2 m from the diffuser. This was done in STAR-CCM+ by making a plane section with a threshold from 2 m to 7.5 m in x-direction as region. A surface average report with temperature as field function was used on this plane section to find the reference temperature. The reference temperature is presented in table 2.

Velocity: Magnitude (m/s)

0.00000   0.074497   0.14899   0.22349   0.29799   0.37248

(a)

Velocity: Magnitude (m/s)

0.00000   0.20096   0.40192   0.60288   0.80384   1.0048

(b)

Figure 35: (a) Plane section 0.02 m above the floor. (b) Plane section normal to the floor at z/H=1

Table 2: Simulations done in STAR-CCM+

Simulation	Height of diffuser [m]	Inlet flow rate [m^3/s]	Heat load [W]	T$_{reference}$ [C]	v$_{max}$ [m/s]	Ar [-]	B [-]
1	0.60	0.036	300	23.5	0.3184	59.7	0.2345
2	0.60	0.036	600	25.2	0.3421	74.9	0.2529
3	0.60	0.054	300	22.6	0.3320	22.9	0.2557
4	0.60	0.054	600	24.1	0.3594	28.9	0.2763
5	0.66	0.036	300	23.4	0.3227	58.8	0.2333
6	0.66	0.036	600	25.2	0.3497	74.9	0.2529
7	0.66	0.054	300	22.5	0.3350	22.5	0.2542
8	0.66	0.054	600	24.1	0.3681	28.9	0.2733
9	0.72	0.036	300	23.5	0.3335	59.7	0.2345
10	0.72	0.036	600	25.2	0.3570	74.9	0.2529
11	0.72	0.054	300	22.6	0.3458	22.9	0.2557
12	0.72	0.054	600	24.2	0.3770	29.3	0.2775

6.2.1 Flow visualization

Figure 35a visualizes the flow from the diffuser at a horizontal plane section 0.02 m above the floor and shows how a typical DV system diffuses its cold air along the floor. Because of the acceleration region near the diffuser, the maximum velocity in the flow along the floor is at around this height. After the flow has reached its maximum velocity, the flow enters the velocity decay region, and the velocity reduces. Figure 35b visualizes the flow from the diffuser at z/H = 1. Here the drop of the flow due to the acceleration region is shown.

6.2.2 Effects of different diffuser height with same simplified Archimedes number

From Table 2 we notice that the reference temperature remains within 0.1°C of similar volumetric flow and heat load when the diffuser height increases, this is visualized in Figure 37. This will give a small change in $\Delta\theta_t$, which is needed when calculating the reduced gravity in Eq. 5, which again will result in a very low difference in the Archimedes number. The Archimedes number is calculated for each simulation and summarized in Table 2. Based on this the height of the diffuser does not influence the Archimedes number, which means that a linear diffuser is independent of the diffuser height. However, this is only within a 20% increase in diffuser height.

Examining the results in Figure 36 we notice that the height has an impact on the maximum velocity, this has been summarized in table 2. We see that with increasing diffuser height, the maximum velocity

increases. This may be due to the increase in diffuser height allowing the gravity in the acceleration region to have more impact on the flow from the diffuser. The results also show that increasing the heat load and the inlet flow rate will increase the maximum velocity. A closer look into the four figures we also notice that the distance between the diffuser and the position of the maximum velocity increases with increasing inlet flow rate. Figure 38 compares the two different inlet flow rates when the height of the diffuser and the heat load is the same, and we see that the distance of the maximum velocity from the diffuser increases by approximately 0.2 m.

In the velocity decay region, which is after the flow has reached its maximum velocity, we see that there is no change between the three different diffuser heights when looking at the four different figures, see Figure 36.

In Figure 37 we see the temperature profiles for all the simulations, 1 m and 5 m from the diffuser. Simulations 3, 7 and 11 resulted in the lowest temperatures, which was expected since the inlet flow rate increased while the heat load was unchanged. Simulations 2, 6 and 10 resulted in the highest temperatures, which also was expected since the heat load increased while the inlet flow rate was unchanged. The results also show that there is little to no temperature difference between the diffuser heights, which has been pointed out earlier.

Discussion

It is important to note that this study was done in steady CFD simulations, and because of limited time the results were obtained as soon as the residuals showed little change. This can have an impact on the results obtained in this study. The inlet boundary was modelled in STAR-CCM+ as an open area, which is not the case for a DV diffuser. The results in this study concerns only a 20% increase in diffuser height.
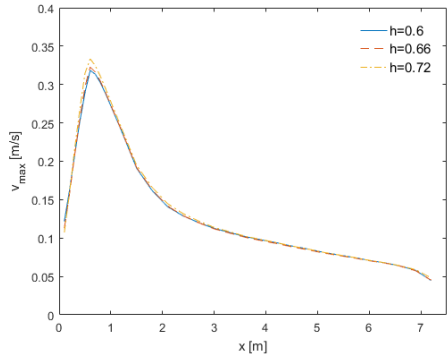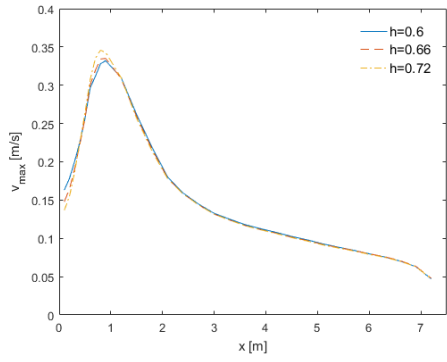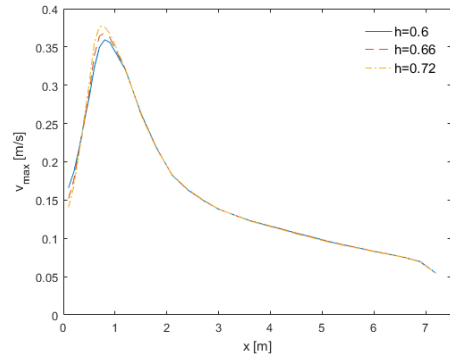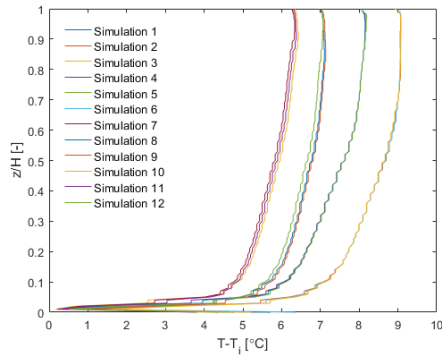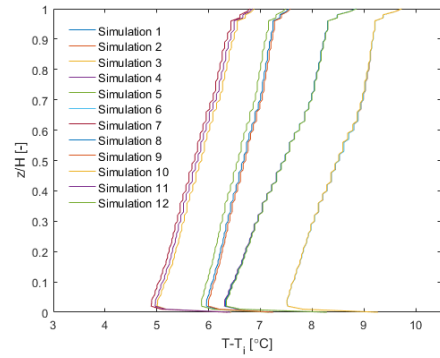
(a)
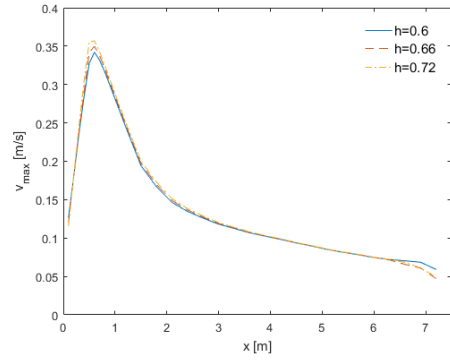
(b)

(c)

(d)

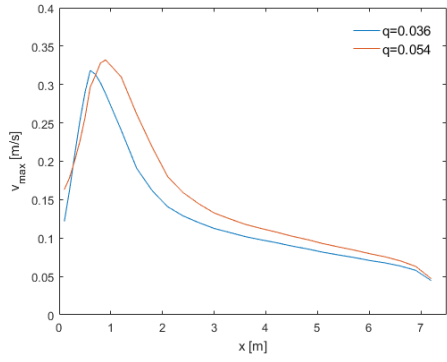Figure 36: Change of Height, same flow rate and heat load

(a) 1 m from the diffuser at z/H=1
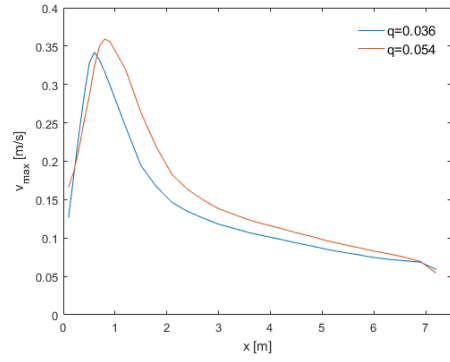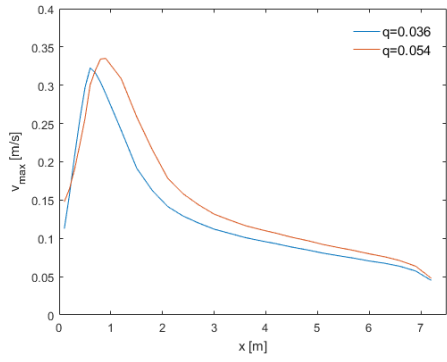
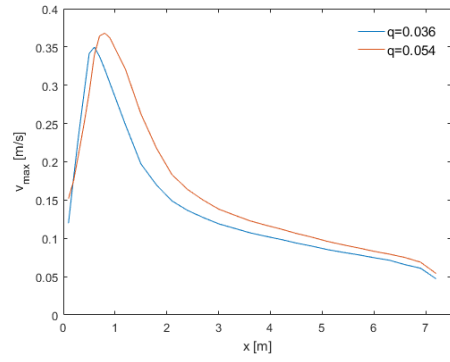(b) 5 m from the diffuser at z/H=5
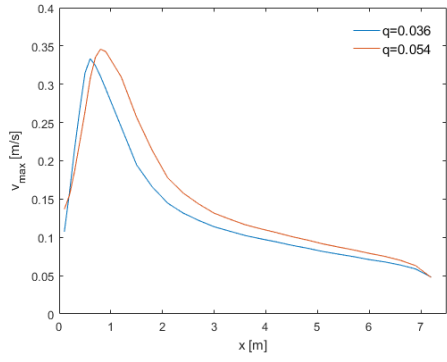
Figure 37: Temperature profiles

(a) h=0.6, Q=300

(b) h=0.6, Q=600
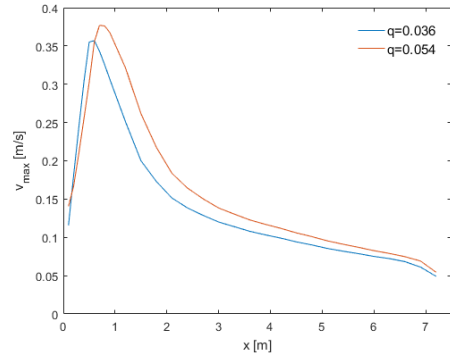
(c) h=0.66, Q=300

(d) h=0.66, Q=600

(e) h=0.72, Q=300

(f) h=0.72, Q=600

Figure 38: Change of flow rate, same height and heat load

7 Conclusion

The objective of the validation chapter, is to compare our simulations from the software with the experimental measurements that were carried out in benchmark. This validation was necessary for the whole study in general. It made it possible for us to verify many parameters that were of great interest throughout the whole work with the CFD. 2D steady-state simulations of a standard benchmark problem were chosen, and performed. The mesh resolution is important and very critical in terms of finding the suitable one that fits the criteria of a particular model. A mesh sensitivity analysis was done with the intention to investigate which one of the meshes that requires refinement. In general, The mesh was refined by selecting trimmer in all of the simulations that were conducted in this study. The simulations led to results where the comparisons of the velocity profiles showed very good agreement with the experimental data.

The general characteristics of DV is presented by simulating 3D cases and results are found in very good agreement with the experiment and numerical results of the literature. It was also observed that a plume is formed above the heat source and stratified zones clearly seen. The flow in this 3D study has shown that the cooler air is in the occupied zone which can then be used to displace the contaminant heat from people and heat sources in the room.

The main objective of this study has been to evaluate what effect different heights of a diffuser has on the Archimedes number proposed in the Nordtest method NT VVS 083. This was done by conducting simulations of a test room with two ventilation openings and a heat source in STAR-CCM+ where the diffuser height, the inlet flow rate and the heat load varied. Dimensions of the test room and the position of the heat loads strictly followed the guidelines of the Nordtest method. The results showed that an increase in diffuser height did not effect the Archimedes number. This is in line with what Skåret proposed, that the Archimedes number for both radial and linear diffusers is independent of the diffuser height. The results are however only within an increase of 20% in diffuser height. Further research is required where the diffuser's height changes, so that we can find out which length parameters should be included in the Archimedes number.

References

[1] The National Human Activity Pattern Survey (NHAPS): A Resource for Assessing Exposure to Environmental Pollutants,https://indoor.lbl.gov/sites/all/files/lbnl-47713.pdf [retrieved 21.05.2018]

[2] Tollef Hjermann, CFD simulation of active displacement ventilation, NTNU,June 2017

[3] Special Applications:Room Air Distribution Systems ,http://machineryequipmentonline.com/hvac-machinery/wp-content/uploads/2016/01/Special-Applications-0118, Date taken 21.05.2018

[4] CBA, http://www.lindab.com/global/pro/products/pages/cba.aspx(Retreieved 21.05.2018)

[5] Displacement Linear Enclosure, http://www.pricecriticalcontrols.com/products/details/dle-displacement-linear-enclosure, date retrieved 21.05.2018.

[6] BT VVS project 1507-00 Universal equations for testing and documenting aerodynamic performance of displacement ventilation units, SINTEFF BYGGFORSK Peter G.Schild et..al., 2003

[7] Air terminal devices: Aerodynamic testing and rating at low velocity Nordtest method NT VVS 083:2003.

[8] Nielsen, P.V.,Stratified flow in a Room with Displacement Ventilation and Wall-Mounted Air Terminal devices. Aalborg: Dept. of Building Technology and Structural Engineering. Indoor Environmental Engineering, No. 85, Vol. R9826,1998.

[9] Hanne Jorunn Trydal, Displacement ventilation in Zero Emission Office Buildings[ZEB],NTNU July 2017.

[10] H Skistad, Displacement Ventilation, Research studies press, John Wiley and Sons, Ltd, West Sussex, UK,1994.

[11] Magnier-Bergeron,L.,Derome,D., and Zmeureuanu,R.,Three-dimensional model of air speed in the secondary zone of displacement ventilation jet. Building and Environment, 114, 483-794,2017.

[12] Versteeg, Malalasekera , An introduction into computational Fluid Dynamics ISBN 0-582-21884-5,1995.

[13] Jérôme Le Dréau,Per Heiselberg,Peter V.Nielsen, DCE Technical Report No.147, Simulation with different turbulence models in an Annex 20 benchmark test using Star-CCM +,Aalborg University,2012.

[14] http://www.cfd-benchmarks.com/benchmarktest/ Retrieved 22.05.2018.

[15] CD-adapco /12.04.010 (Star ccm+)

[16] Lard Davidson, Ventilation by Displacement in a Three-Dimensional Room. A Numerical Study Vol 24, No4, pp, 363-373, 1989.

[17] http://www.cfd-benchmarks.com/

[18] S. Gilani, H. Montazeri, B. Blocken, CFD simulation of stratified indoor environment in displacement ventilation: Validation and sensitivity analysis, Build. Environ. 95 (2016) 299-313